

IVS contribution to ITRF2014

Sabine Bachmann¹ · Daniela Thaller¹ · Ole Roggenbuck^{1,3} · Michael Lösler² ·
Linda Messerschmitt¹

Received: 25 September 2015 / Accepted: 14 March 2016 / Published online: 5 April 2016
© Springer-Verlag Berlin Heidelberg 2016

Abstract Every few years the International Terrestrial Reference System (ITRS) Center of the International Earth Rotation and Reference Systems Service (IERS) decides to generate a new version of the International Terrestrial Reference Frame (ITRF). For the upcoming ITRF2014 the official contribution of the International VLBI Service for Geodesy and Astrometry (IVS) comprises 5796 combined sessions in SINEX file format from 1979.6 to 2015.0 containing 158 stations, overall. Nine AC contributions were included in the combination process, using five different software packages. Station coordinate time series of the combined solution show an overall repeatability of 3.3 mm for the north, 4.3 mm for the east and 7.5 mm for the height component over all stations. The minimum repeatabilities are 1.5 mm for north, 2.1 mm for east and 2.9 mm for height. One of the important differences between the IVS contribution to the ITRF2014

and the routine IVS combination is the omission of the correction for non-tidal atmospheric pressure loading (NTAL). Comparisons between the amplitudes of the annual signals derived by the VLBI observations and the annual signals from an NTAL model show that for some stations, NTAL has a high impact on station height variation. For other stations, the effect of NTAL is low. Occasionally other loading effects have a higher influence (e.g. continental water storage loading). External comparisons of the scale parameter between the VTRF2014 (a TRF based on combined VLBI solutions), DTRF2008 (DGFI-TUM realization of ITRS) and ITRF2008 revealed a significant difference in the scale. A scale difference of 0.11 ppb (i.e. 0.7 mm on the Earth's surface) has been detected between the VTRF2014 and the DTRF-2008, and a scale difference of 0.44 ppb (i.e. 2.8 mm on the Earth's surface) between the VTRF2014 and ITRF2008. Internal comparisons between the EOP of the combined solution and the individual solutions from the AC contributions show a WRMS in X- and Y-Pole between 40 and 100 μ s and for dUT1 between 5 and 15 μ s. External comparisons with respect to the IERS-08-C04 series show a WRMS of 132 and 143 μ s for X- and Y-Pole, respectively, and 13 μ s for dUT.

✉ Sabine Bachmann
sabine.bachmann@bkg.bund.de

Ole Roggenbuck
ole.roggenbuck@jade-hs.de

Michael Lösler
michael.loesler@fb1.fra-uas.de

¹ Federal Agency for Cartography and Geodesy,
Richard-Strauss-Allee 11, 60598 Frankfurt am Main,
Germany

² Faculty of Architecture, Civil Engineering and Geomatics,
Laboratory for Industrial Metrology, Frankfurt University of
Applied Sciences, Nibelungenplatz 1, 60318 Frankfurt am
Main, Germany

³ Present Address: Institute of Metrology and Analysis
Technique, Jade Hochschule
Wilhelmshaven/Oldenburg/Elsfleth, Friedrich-Paffrath-Str.
101, 26389 Wilhelmshaven, Germany

Keywords ITRF2014 · VLBI · Intra-technique
combination · Station coordinates · Terrestrial reference
frame · Earth orientation parameters

1 Introduction

In February 2013, the International Terrestrial Reference System (ITRS) Center of the International Earth Rotation and Reference Systems Service (IERS) sent out a Call for Participation for the next International Terrestrial Reference Frame

(ITRF).¹ All four services representing the space geodetic techniques—Doppler Orbitography and Radiopositioning Integrated by Satellite (DORIS), Global Navigation Satellite Systems (GNSS), Satellite Laser Ranging (SLR) and Very Long Baseline Interferometry (VLBI)—were requested to submit contributions to the generation of the ITRF2014. Similar to ITRF2008 and other preceding ITRFs, ITRF2014 will be an inter-technique combined product that consolidates the products of each space geodetic technique (Altamimi et al. 2011). The contributions of the different techniques are diverse: GNSS data contain daily solutions, DORIS and SLR data contain weekly solutions and VLBI data contain session-wise datum-free normal equations. Since ITRF2005, the VLBI contribution has consisted of normal equations derived from a combination of different individual contributions from the IVS Analysis Centers (Vennebusch et al. 2007). The same strategy was utilized for ITRF2008 (Böckmann et al. 2010b) and ITRF2014. The development procedure for the VLBI combination has been continuously refined with an increasing number of individual contributions. The VLBI data are provided by the International VLBI Service for Geodesy and Astrometry (IVS) (Schlüter and Behrend 2007), which is organized under the umbrella of the International Association of Geodesy (IAG) and the International Astronomical Union (IAU), and contributes to the IERS. Since ITRF2008, six years of additional observations have become available, including new sites in the continuously evolving network (Behrend et al. 2008). In this paper, we describe the combination process of the VLBI contribution to ITRF2014, which also resembles the current state-of-the-art product of combined VLBI solutions. We are focusing on station positions and Earth Orientation Parameters (EOP). We will show the benefit of the combination of products by comparing the individual contributions and by validating to external products such as DTRF2008, ITRF2008 and C04 EOP time series. We also identified deficiencies in the processing chain, which currently deteriorate the precision of our best solution and we will show that the primary limiting factor is the impact of a week network configuration on the scale parameter for global VTRF solutions followed by systematic differences in the EOP analysis and the impact of correlations between the AC contributions. Comparisons of the scale parameter complete the work, since VLBI and SLR are presently the only two space geodetic techniques that are contributing to the scale of the ITRF. Overall, 5796 combined sessions have been submitted to the IERS ITRS Center as IVS contribution to the ITRF-2014.

The analysis standards as well as the session characteristics used as input for the combination are described in Sect. 2. The combination process for the different solution

types is described in Sect. 3. Results related to station coordinates are shown in Sect. 4 and results related to EOPs in Sect. 5. A summary of this paper and a conclusion is given in Sect. 6.

The data DOI 10.5880/GFZ.1.1.2015.002 has been assigned to the IVS contribution to ITRF2014 (cf. Nothnagel 2015). A presentation covering this subject can be found in Heinkelmann et al. (2013). This citation is included in the metadata imbedded within the cited data. For the IVS contribution to ITRF2014, this data collection appreciation extends to the whole chain of data acquisition: VLBI stations, correlators, data centers, data analysis centers and combination centers. The static dataset in form of SINEX files has been established as open access in the three IVS data centers.^{2,3,4} The landing page containing links to the dataset, a description of the dataset and the accompanying metadata was established at the IVS Combination Center website: <http://ccivs.bkg.bund.de/doi>.

2 Input contributions

The basis of the combination process are VLBI observations, which are organized in sessions over a certain time span with a defined start and end time. These raw data are transferred from each station to a dedicated correlator, which generates time delay input data for the analysis of the experiment. The fundamentals of the VLBI cross-correlation procedure can be found in, e.g. the articles series in Thomas (1972a, b, 1973).

2.1 VLBI session characteristics and analysis standards

For the IVS contribution to the ITRF2014, only 24-h sessions are used. In contrast to the regular rapid solution where only R1 and R4 sessions are used, the IVS contribution to ITRF-2014 contains all 24-h sessions. All VLBI sessions, including the sessions that are used for the ITRF2014 contribution, can be found in the IVS master schedule.⁵ The IVS Analysis Centers (ACs) are advised to make use of (at least) all R1 and R4 sessions through 31 December 2014, with contributing ACs responsible for the delivery of the sessions. ACs contributing to operational combination EOP products not necessarily submit a contribution to the IVS combination for the ITRF2014. However, contributing to the IVS is open to every interested institute, implying that their contribution is in the correct format. The input contributions are normal

² ftp://ivs.bkg.bund.de/pub/vlbi/ITRF2014/daily_sinex/ivs2014a/.

³ ftp://ivsopar.obspm.fr/vlbi/ITRF2014/daily_sinex/ivs2014a/.

⁴ ftp://cddis.gsfc.nasa.gov/pub/vlbi/ITRF2014/daily_sinex/ivs2014a/.

⁵ <ftp://ivs.bkg.bund.de/pub/vlbi/ivscontrol/>.

¹ IERS Message No. 225 in <http://www.iers.org/Messages>.

Table 1 IVS analysis centers and their contribution to operational IVS products and to the ITRF2014

AC	Name	Software	Operational AC	ITRF2014	
				Submitted	Included
AUS	Geoscience Australia, Australia	OCCAM (LSC)	No	Yes	No
BKG	Federal Agency for Cartography and Geodesy, Germany	Calc/(nu)Solve	Yes	Yes	Yes
CGS	Centro di Geodesia Spaziale, Italy	Calc/(nu)Solve	Under review	Yes	Yes
DGFI-TUM	German Geodetic Research Institute/Technical University of Munich	OCCAM (LSM)	Yes	No	No
GFZ	German Research Center for Geosciences	VieVS@GFZ	Under review	Yes	Yes
GSFC	Goddard Space Flight Center, USA	Calc/(nu)Solve	Yes	Yes	Yes
IAA	Institute of Applied Astrometry, Russia	Quasar	Yes	Yes	Yes
NMA	Norwegian Mapping Authority, Norway	GEOSAT	No	Yes	No
OPAR	Observatory of Paris, France	Calc/(nu)Solve	Yes	Yes	Yes
SHAO	Shanghai Observatory, China	Calc/(nu)Solve	No	Yes	Yes
USNO	US Naval Observatory, USA	Calc/(nu)Solve	Yes	Yes	Yes
VIE	Vienna University of Technology, Austria	VieVS	No	Yes	Yes

equations stored in the SINEX⁶ file format, containing station coordinates and EOP, i.e., pole coordinates (including rates), universal time, LOD and nutation.

Table 1 shows the ACs contributing to the IVS. It is indicated to which product they are contributing and which software is used to analyze the sessions. Five ACs contribute solutions to the ITRF2014 although they do not contribute to the operational combined product. Several new and independent software packages have also been used. For ITRF2008, seven ACs using four different software packages contributed to the combined solution. Now, ten ACs using five different software packages contributed to the combined solution for ITRF2014.

As the choice of sessions is up to the Analysis Center, no standard list of required sessions was circulated and the submitted amount of sessions differ. Figure 1 shows the time line of the submitted contributions by each AC and the total number of contributed sessions. Most of the ACs submitted analyzed data going back to the late 1970s. Only BKG, CGS and USNO started session analysis in 1984, leaving out the early sessions.

Reliable combined results can only be generated if all contributions from the different ACs are consistently analyzed using common conventions and models. Table 2 summarizes the common standards for the VLBI analysis for the ITRF2014 contribution, which have been distributed by the IVS Analysis Coordinator.⁷ On the right-hand side, the standards used for the IVS ITRF2008 contribu-

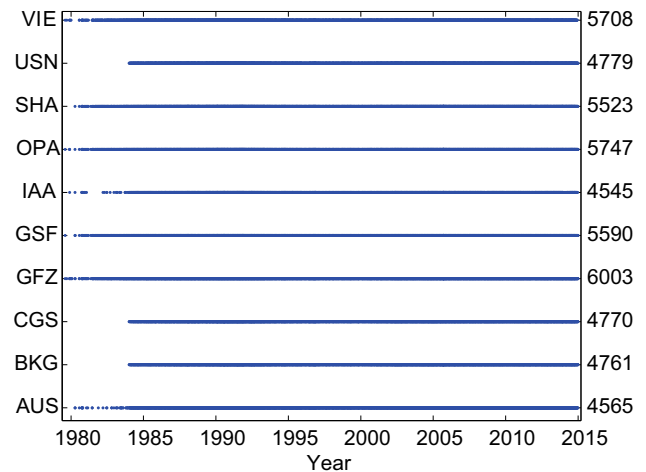


Fig. 1 SINEX file availability for the different ACs over time. The total amount of contributed SINEX files for each AC is indicated on the right hand side

tion are listed for comparison. Significant differences are the IERS Conventions 2010 (Petit and Luzum 2010) instead of IERS Conventions 2003 (McCarthy and Petit 2003) (e.g. IAU2006A instead of IAU2000A Nutation model), an ITRF-2014-specific eccentricities file that is slightly different from the conventional IVS analysis file and the a priori source position handling. For the IVS contribution to ITRF2008, the ICRF1 and ICRF-Ext.1 were used as well as CRS realizations of the ACs (Böckmann et al. 2010b). For the ITRF2014 contribution ICRF2 (Fey et al. 2009, 2015) defining sources are constrained to a priori positions as defined by ICRF2 and special handling sources are treated as arc-parameters. For all other sources, both possibilities are allowed.

⁶ <http://www.iers.org/sinex>.

⁷ http://lupus.gsfc.nasa.gov/files_IVS-AC/ITRF2013_checklist_v2014Feb07.pdf.

Table 2 Analysis standards for IVS contribution to the ITRF2014 and the corresponding standards used for the IVS contribution to ITRF2008

	Standard	ITRF2014	ITRF2008	
Modeling	Station coordinate			
	Solid Earth tide	IERS conventions 2010, following Mathews et al. (1997)	IERS conventions 2003, following Mathews et al. (1997)	
	Permanent tide	Conventional tide free	Conventional tide free	
	Love numbers	h2 (freq = 0) = 0.6078 l2 (freq = 0) = 0.0847	h2 (freq = 0) = 0.6078 l2 (freq = 0) = 0.0847	
	Ocean loading	TPX07.2 ^a (Egbert et al. 1994) or FES2004	FES2004 ^b (Lyard et al. 2006) without correction for geocenter motion	
	Pole tides	IERS conventions 2010	IERS conventions 2003	
	Atmosphere pressure loading	None	None	
	Other loading effects	None	None	
	Troposphere			
	Zenith hydrostatic delay	Modified Saastamoinen (Davis et al. 1985)	Modified Saastamoinen (Davis et al. 1985)	
	Pressure and temperature	From database or VMF values interpolated to epoch	From database with pressure measured at the site	
	Dry mapping function	Dry VMF1 (Böhm et al. 2006)	Dry VMF1	
	Gradient a priori	Latest DAO results ^c (Schubert et al. 1993 ; MacMillan and Ma 1997)	AC dependent (numerical weather model or zero)	
	Antenna and station			
	Axis offsets	IVS ITRF2014 axis offset information file ^d	IVS analysis conventions (Nothnagel 2009)	
	Thermal expansion	IVS analysis conventions (Nothnagel 2009)	IVS analysis conventions (Nothnagel 2009)	
	Eccentricities	IVS ITRF2014 eccentricities ^e	Official IVS table ^f	
	Earth orientation parameters			
	Tidal variations in X , Y , $dUT1$	IERS conventions 2010, include Hi-freq libration terms	IERS conventions 2003	
	Nutation	IAU2006 (without free core nutation)	IAU2000A (without free core nutation)	
	Miscellaneous			
	Relativistic scale	IERS conventions 2010	IERS conventions 2003	
	Shapiro effect	IERS conventions 2010	IERS conventions 2003	
	Estimates	Troposphere		
		Wet mapping function	Wet VMF1	Wet VMF1
		Gradient	Chen–Herring gradients (Chen and Herring 1997)	MacMillan (1995) with wet VMF1
		Sources		
Defining sources		Constrain to a priori positions of ICRF2 ^g	Constrain to a priori positions of ICRF-Ext.1 ^h and individual CRS realizations by the ACs, with a varying number of datum sources (Böckmann et al. 2010b)	
Special handling sources		Treat as arc-parameters (squeeze out)		
Other sources		Either constrain to ICRF2 positions or treat as arc-parameters and squeeze out		
Parameterization				
TRF		All XYZ components of all sites	All XYZ components of all sites	
EOP (24 h sessions)		All EOP components: XP , YP , $UT1$ -TAI, XP -rate, YP -rate, LOD , Nutation X and Y		

The upper part contains the standards for the modeling, the lower part for the estimates

^a <http://volkov.oce.orst.edu/tides/TPX07.2.html>

^b http://lupus.gsfc.nasa.gov/files_IVS-AC/gsfcdao_gmao.mgr

^c ftp://ftp.legos.obs-mip.fr/pub/soa/maree/tide_model/global_solution/fes2004/

^d http://lupus.gsfc.nasa.gov/files_IVS-AC/gsfcdat_itrf2013.axo

^e http://gemini.gsfc.nasa.gov/solve_save/ECCDAT_itrf2013.ecc

^f http://gemini.gsfc.nasa.gov/solve_save/ECCDAT.ecc

^g <http://hpiers.obspm.fr/webiers/icrf2/icrf2.html>

^h <https://hpiers.obspm.fr/icrs-pc/icrf/icrf-ext1.html>

2.2 VLBI network

The VLBI network consists of radio telescopes on geodetic or astronomic observation sites in different countries, distributed worldwide. A world map indicating the location of the sites with VLBI telescopes is shown in Fig. 2. In areas, such as Western Europe, North America and Japan, more telescopes are situated, while in remote areas including Antarctica, the polar regions, and areas such as South America, Africa or Eastern Europe, sites with VLBI telescopes are sparsely distributed. Combined VLBI sessions contain all stations, which participated in the IVS observing program. For the long-

term terrestrial reference frame based on VLBI observations (VTRF) only stations which are stable in their position and with a sufficient number of observed sessions are included.

In Fig. 3 the participation of VLBI telescopes is shown for the complete time span of the ITRF2014 data. For a better readability, only stations with more than ten successfully combined sessions are shown. For VTRF datum definition only stations with a long and stable observation period (without earthquakes) are used.

The coordinate and velocity modeling of these stations is described in Sect. 3.3. The estimation of the station coordinates is the result of adding normal equations of multiple

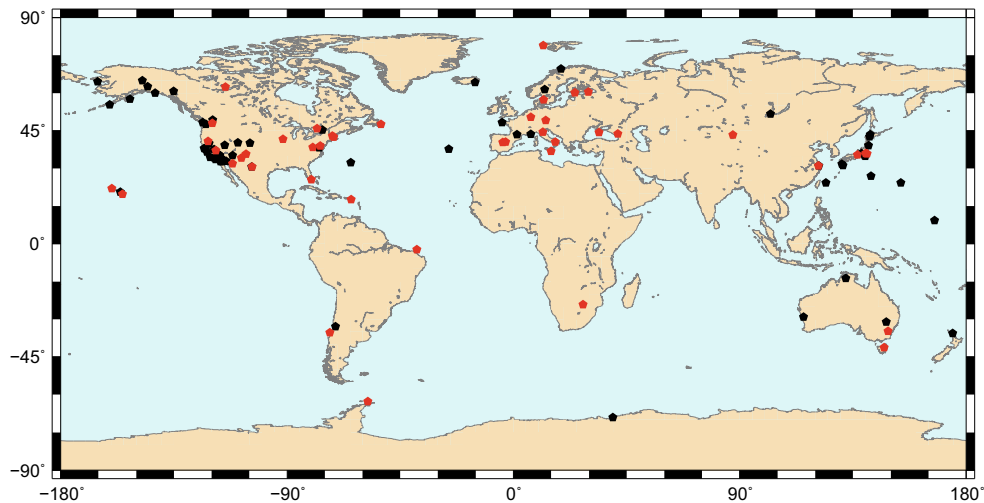


Fig. 2 Global distribution of VLBI stations (red = datum station)

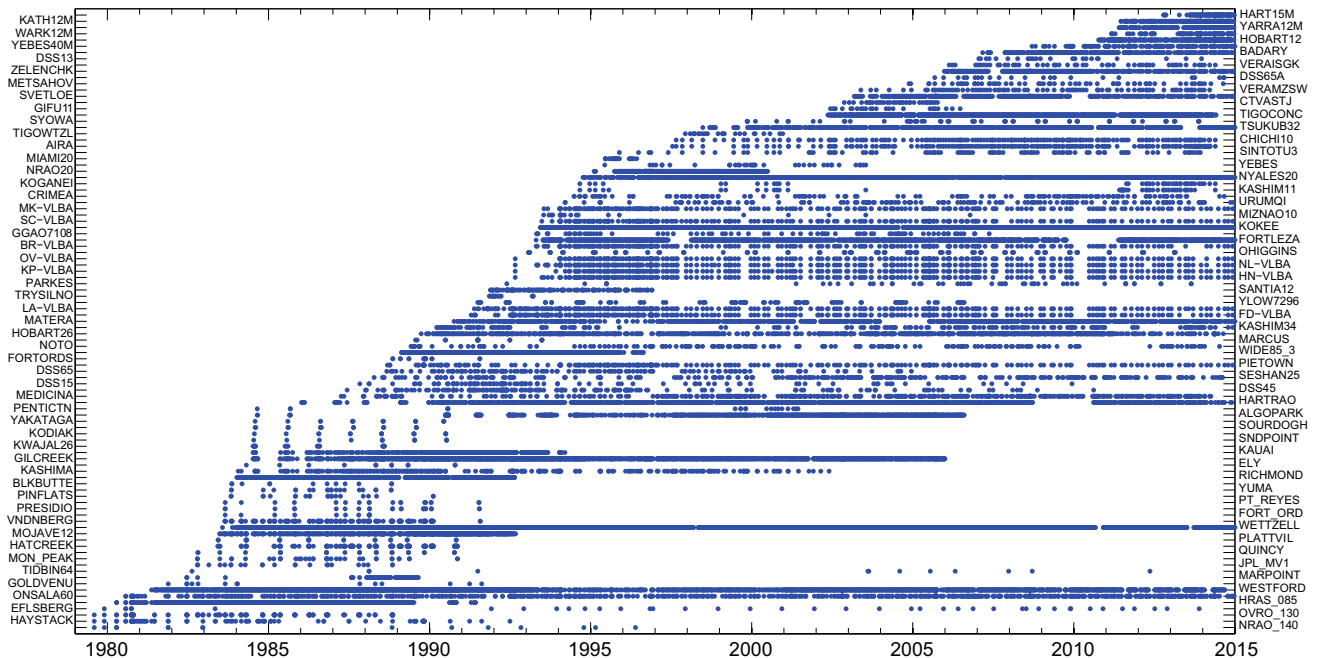


Fig. 3 Station participation in VLBI sessions until 2015. Only stations with more than ten observed sessions are shown

sessions with respect to a given epoch. Velocities are determined by estimating the coordinate differences of one station over a certain time span.

3 Combination strategy

The combination strategy comprises the homogenization of the individual contributions, quality testing and the calculation of a combined solution by stacking the individual contributions. Particular attention is paid to outlier detection and weighting strategies. Each AC contribution is weighted using a dedicated strategy to best use the individual contributions in the combined solution (cf. Sect. 3.2.2).

3.1 Session-wise combination process

The combination is based upon session-wise SINEX files containing datum-free normal equations for station coordinates and EOP (for ITRF contribution) as well as additional source positions for routine combination. In the following paragraphs, a short description of the general combination procedure will be given, highlighting major analytic differences that have been introduced since the IVS contribution to ITRF2008. The interested reader is referred to Böckmann et al. (2010c) for a detailed description of the combination methodology used for ITRF2008 contribution. Figure 4 shows the general processing strategy of the combination, in which the first step is an epoch transformation on the same epoch for every contribution. For the ITRF2014 contribution, the IVS decided—for the first time—to transform each session to 12 h UT, instead of mid-session like for operational IVS combination, to conform with the other space geodetic techniques.

The second step of the combination processing strategy is a transformation to equal a priori station coordinates. Precise a priori values are important for the quality and reliability of the combination result. The a priori values for station coordinates are taken from the latest combined long-term (quarterly) solution, which is the one with the most up-to-date global VLBI solutions available. Since different incidents such as earthquakes or station repairs lead to non-linear antenna displacements, the prompt determination of accurate station positions is needed. This is also the case for newly built telescopes. Section 3.3 describes the strategy of the VTRF generation.

The next step of the session-wise combination includes an outlier test for station coordinates. In this step, major changes have been applied compared to the precedent procedure for ITRF2008. For ITRF2008, contributions were rejected as outliers in station position if the following two criteria were met (from Böckmann et al. 2010b):

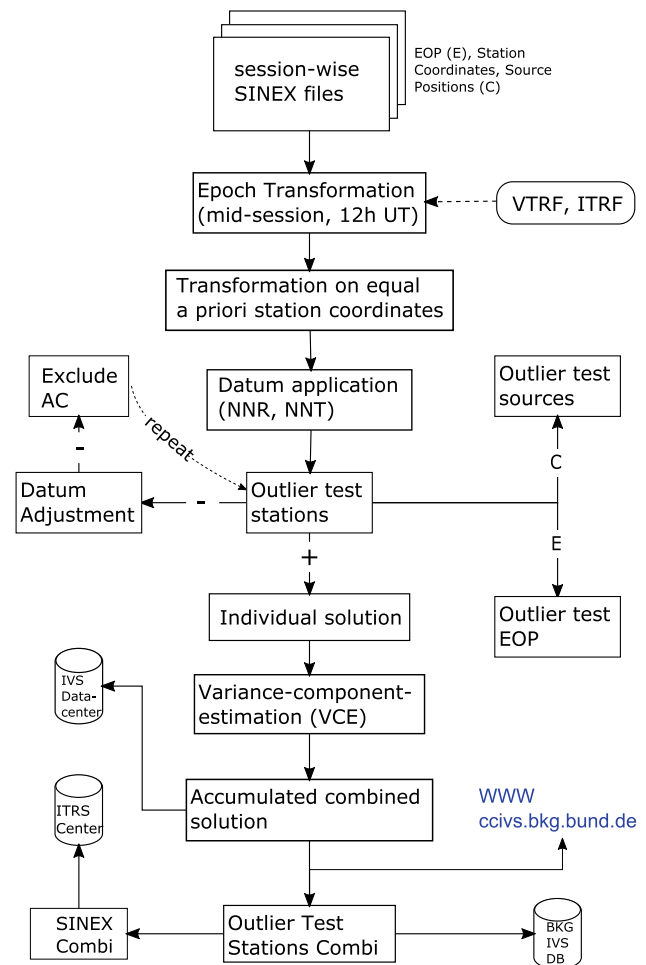


Fig. 4 Combination strategy

1. the correction to the a priori position was larger than 5 cm in the horizontal and 7.5 cm in the vertical component, and
2. the parameter correction was larger than three times its formal solution error.

This static approach has been replaced by a dynamic approach using the Least Median of Square method (LMS) described in detail in Sect. 3.2.1. Based on normal equations with identical epochs and identical a priori values, the individual solution for each AC is generated. Comparing these individual solutions, a weighting factor is determined using a variance component estimation (VCE) (see Sect. 3.2.3 for details). The combined normal equation is generated by accumulating the weighted contributions of the ACs. Applying no-net rotation (NNR) and no-net translation (NNT) conditions for station coordinates removes the datum defect of the normal equations and allows its inversion. Stations, where no reliable coordinates can be determined for specific sessions falling in a particular time span (e.g. by reason of station displacements due to earthquakes, maintenance work

at the antenna, or too few observations), are excluded from the datum definition and treated as free parameters. As soon as these stations are again stable enough to determine a reliable station coordinate, they are used as datum stations. A SINEX file containing the datum-free normal equations of the combined solution is then submitted to the IERS ITRS Center and the IVS data center.⁸

3.2 Outlier detection and weighting strategy

Outlier detection plays an important role within the IVS combination. Treating outliers straddles a fine line between keeping data heterogeneity and elimination of real outliers. Although the original data are the same for all contributing ACs, the solutions show differences due to analysis software characteristics.

Robust outlier detection based on the Least Median of Squares (LMS) method is used within the IVS combination. This method allows reliable outlier detection with a small number of input parameters and will be described in Sect. 3.2.1.

A similar problem arises for the weighting of the individual contributions within the combination process. The VCE is used to derive the weighting factor for each AC. The weighting strategy used for the combination process is described in Sect. 3.2.2 and the VCE in Sect. 3.2.3.

3.2.1 Least median of squares

The usage of common least-squares techniques requires a gross-error free observation set to get a likely estimation. Gross errors in observations bias the estimator. Hence, robust estimators are developed to reduce the influence of contaminated observations on the estimated parameters. The robustness of an estimator is indicated by the so-called breakdown point of the estimator that describes the rate of outliers the estimator can handle before it fails. The maximum value of the breakdown point is 50 % but in practice, this value is mostly not reached, e.g. in case of a leverage observation.

In geodesy most of the robust estimators are based on so-called M-estimators and are solved iteratively by re-weighted least-squares (cf. Jäger 2005, pp. 113ff). Kutterer et al. (2003) evaluate different modified M-estimators used in the analysis of VLBI data. The breakdown point of such an estimator is about 10–40 % (e.g. Neitzel 2003; Salvini 2008). During the pre-processing of the combination, the comparable data are limited to the number of contributing ACs. Hence, only a consistency check of EOPs and station coordinates can be carried out. An estimator, however, must be suitable to derive unbiased parameters from a small and in some cases

partially contaminated set of observations. The (modified) M-estimators do not meet these requirements.

Another approach comes from the combinatorial analysis. Rousseeuw (1984) combines the high breakdown point of 50 % of the median with a permutation strategy of observations. Instead of using the complete set of n observations \mathbf{I} , only a subset of $n_l = u$ observations \mathbf{I}_l is used to estimate the u parameters \mathbf{x}_l . Based on the l th solution \mathbf{x}_l the corresponding vector of n residuals \mathbf{v}_l as well as the median of the squared residuals are estimated. The estimated u parameters \mathbf{x}_l are unambiguous because this solution is based on a non-redundant subset \mathbf{I}_l of \mathbf{I} . This estimation process is repeated for all $l = 1 \dots \binom{n}{u}$ permutations \mathbf{I}_l that solve the parameters unambiguously. The robust solution of the estimated parameters \mathbf{x}_{LMS} is indicated by the l th subset that provides the minimal median of the squared residuals. The objective function of the so-called least median of squares (LMS) is given by

$$\Omega = \min_l \text{med } \mathbf{v}_l^2$$

The LMS reaches a breakdown point of 50 % asymptotically (Jäger 2005, p. 133). The estimated parameters \mathbf{x}_{LMS} are only based on the u observations of the corresponding subset. In case of an outlier free observation set, $n - u$ observations are unfoundedly rejected. Thus, in most applications the robust solution of the LMS is introduced to a re-weighting least-squares method (e.g. Lösler 2011). Based on the estimated parameters \mathbf{x}_{LMS} the initial weights \mathbf{w} are derived by comparing the robust standardized residuals to a carefully selected threshold k , e.g. $k = 3$ according to the 3σ rule.

$$w_i = \begin{cases} 1, & \text{if } |v_i| \leq k\sigma_{LMS} \\ 0, & \text{else} \end{cases}$$

Here, σ_{LMS}^2 describes a robust estimation of the variance of the unit weights

$$\sigma_{LMS}^2 = \frac{1}{\Phi^{-1}(0.75)} \left(1 + \frac{5}{n-u} \right) \sqrt{\Omega},$$

where Φ denotes the standard normal cumulative distribution and $1 + \frac{5}{n-u}$ is an additional scaling term to avoid an underestimation in case of a small degree of freedom $n - u$ (Rousseeuw and Leroy 2003). During the adjustment process of the re-weighted least-squares an improved estimation

$$\hat{\sigma}_0 = \frac{\sum_{i=1}^n w_i v_i^2}{\sum_{i=1}^n w_i - u}$$

of σ_{LMS}^2 is introduced for deriving weights for the observations.

⁸ ftp://ivs.bkg.bund.de/pub/vlbi/ITRF2014/daily_sinex/ivs2014a/.

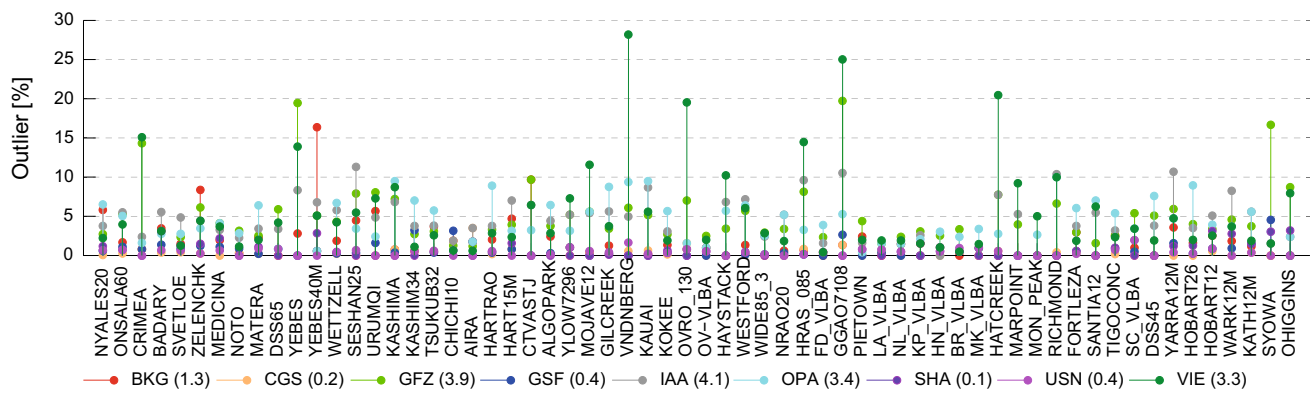


Fig. 5 Outliers for stations with more than 30 observed sessions and more than five outliers for each AC in percent with respect to the total number of combined sessions per station. The *numbers* behind the AC name indicate the median of outliers over all stations (%)

Comparing the outlier test described above with the outlier test applied for the IVS contribution to the ITRF2008 (cf. Böckmann et al. 2010b), the outlier test became independent of the station a priori values. Fixed thresholds for station corrections to their a priori values (5 cm in horizontal and 7.5 cm in vertical component, cf. Sect. 3.1) are replaced by absolute differences of the station coordinates with respect to the median found using the LMS. For the IVS contribution to the ITRF2014, mean values of the absolute differences reported for the detected outliers are 3.7 cm for north, 2.8 cm for east and 6.0 cm for height component. If outliers are detected and the parameters are rendered incorrect, the associated AC will be excluded from the combination for the specific session.

Figure 5 shows station outliers for each AC considering stations with more than 30 observed sessions and more than five detected outliers per station and AC. The outliers are expressed in percent with respect to the number of combined sessions per station. The median of the number of outliers over all stations (in %) is given in parentheses for each AC in the legend. Comparing the median and analyzing the graphs of Fig. 5 allows the identification of two groups of outliers within the ACs: one group of 0.1–0.4 % and a second group of 1.3–4.1 %. A relation to the software packages used for the analysis is not clearly visible since similar software packages are represented in both groups (see also Table 1).

The general assumption of the VLBI combination is that using different analysis strategies reduces the correlations within the contribution. Analyzing the results in Fig. 5, raises the question if the analysis strategies differ sufficiently to keep the correlation at the lowest level possible. The impact on correlated AC contributions has been evaluated in a pilot study in Böckmann et al. (2010a). This has to be studied in detail since an increase of ACs is expected in the future.

3.2.2 Weighting strategies

Though the input data are similar, the ACs are producing independently generated solutions. Consequently, no correlations between the individual solutions of the ACs in terms of cofactor matrices are given. Individual (group) weighting factors are introduced via variance component estimation (see Förstner 1979). Two approaches of a VCE are applicable: (1) with respect to the observation (VCEO), and (2) with respect to pseudo-observations (VCEP). A detailed description of both procedures can be found in Bachmann and Lösler (2012). For the group definition every AC can be defined as one group, or alternatively, groups are defined by gathering ACs which use the same software package, taking into account similarities between analysis software used by the ACs. The VCEP approach better reflects the effective influence of the analyzed data; however, the convergence of result is less reliable as for the VCEO and often fails. This yields to unrealistic and unreliable high values for weighting factors and unbalanced distribution of weighting factors between the contributing ACs for the concerned session. Both approaches are implemented within the IVS combination. The VCEP approach is applied for the routine rapid combination as it was found empirically that it better reflects the real proportion of the influences of the data input.

For the ITRF2014 contribution, the VCEO was applied to stabilize the weighting procedure of the different ACs. VCEO is a distorted estimator leading to overly optimistic results since the degrees of freedom are increased artificially. It became apparent that the convergence of the VCEO is more stable than for the VCEP, which leads to more homogeneous weights between the ACs. Especially, sessions with a small number of stations and/or weak network geometry lead to unrealistic high weights, independent of the software used by the ACs. This is surprising as both methods are expected to provide equally reliable results. Further investigations will

be done to clarify these inconsistencies. The VCEO applied for the IVS ITRF2014 contribution is described in detail in the next section.

3.2.3 Variance component estimation with respect to the observations (VCEO)

Förstner (1979) proposes a method to estimate variance components of observation sets which are stochastically independent. The observation vector \mathbf{l} that contains m observation sets \mathbf{l}_j is given by

$$\mathbf{l} = (\mathbf{l}_1^T \mathbf{l}_2^T \dots \mathbf{l}_m^T)^T.$$

If \mathbf{l}_j are assumed as uncorrelated, the stochastic model reads

$$\mathbf{C} = \sigma_1^2 \begin{bmatrix} \mathbf{C}_1 & \mathbf{0} & \dots & \mathbf{0} \\ \mathbf{0} & \mathbf{0} & & \\ \vdots & & \ddots & \vdots \\ \mathbf{0} & & \dots & \mathbf{0} \end{bmatrix} + \sigma_j^2 \begin{bmatrix} \mathbf{0} & \mathbf{0} & \dots & \mathbf{0} \\ \mathbf{0} & \mathbf{C}_j & & \\ \vdots & & & \vdots \\ \mathbf{0} & & \dots & \mathbf{0} \end{bmatrix} + \dots + \sigma_m^2 \begin{bmatrix} \mathbf{0} & & \dots & \mathbf{0} \\ & \ddots & & \vdots \\ \vdots & & \mathbf{0} & \mathbf{0} \\ \mathbf{0} & \dots & \mathbf{0} & \mathbf{C}_m \end{bmatrix},$$

where σ_j^2 and \mathbf{C}_j denote the unknown variance factor and the variance–covariance matrix of the j th observation set \mathbf{l}_j , respectively. The normal equation system of the combined solution is

$$\mathbf{x} = (\mathbf{A}^T \mathbf{C}^{-1} \mathbf{A})^{-1} \mathbf{A}^T \mathbf{C}^{-1} \mathbf{l} = \mathbf{N}^{-1} \mathbf{n},$$

where \mathbf{A} denotes the Jacobian matrix, which contains the partial derivatives with respect to the unknown parameters \mathbf{x} and \mathbf{n} as well as \mathbf{N} represent the normal equation vector and matrix, respectively. The estimation of the j th unknown variance component is (Jäger 2005, pp. 227ff)

$$\begin{aligned} \sigma_j^2 &= \frac{\mathbf{v}_j^T \mathbf{C}_j^{-1} \mathbf{v}_j}{r_j} = \frac{(\mathbf{A}_j^T \mathbf{x} - \mathbf{l}_j)^T \mathbf{C}_j^{-1} (\mathbf{A}_j^T \mathbf{x} - \mathbf{l}_j)}{n_j - \text{trace}(\mathbf{N}^{-1} \mathbf{A}_j^T \mathbf{C}_j^{-1} \mathbf{A}_j)} \\ &= \frac{\mathbf{x}^T \mathbf{N}_j \mathbf{x} - 2 \mathbf{x}^T \mathbf{n}_j + \mathbf{l}_j^T \mathbf{C}_j^{-1} \mathbf{l}_j}{n_j - \text{trace}(\mathbf{N}^{-1} \mathbf{N}_j)}. \end{aligned} \tag{1}$$

Here, r_j is the redundancy, n_j is the number of observations given in \mathbf{l}_j and the vector \mathbf{v}_j contains the residuals of the j th observation set.

Förstner’s method can be applied whenever the j th part of the normal equation system $\mathbf{N}_j \mathbf{x}_j = \mathbf{n}_j$, the weighted sum of (reduced) observations $\mathbf{l}_j^T \mathbf{C}_j^{-1} \mathbf{l}_j$ as well as the number of observations n_j are given. A strong benefit of Eq. (1) is that

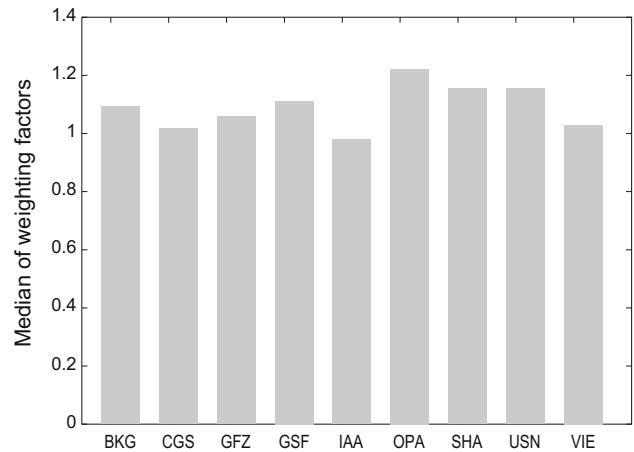


Fig. 6 Median of the individual weighting factors of the ACs

deeper knowledge of the implemented functional model \mathbf{A} , the individual weighting strategy and the used observations \mathbf{l}_j is not necessary and usually not known on the level of combination. These conditions are fulfilled using the m individual AC contributions given in respective SINEX files.

Finally, a weighting factor λ_j is computed for each AC and session as reciprocal value of σ_j :

$$\lambda_j = \frac{1}{\sigma_j^2}$$

The median of the individual AC weighting factor resulting from the VCE is shown in Fig. 6. Smoothed time series of the different weighting factors for the ACs are shown in Fig. 7.

The weighting factors vary between about 1 and 1.4 with local irregularities for some ACs. Figure 7 clearly shows an annual signal for GFZ and VIE ACs, which are using the VLBI analysis software VieVS and VieVS@GFZ, respectively (see Böhm et al. 2012)⁹ (see also Table 1).

Investigations at GFZ revealed that the reason for the annual signal can be found in National Geodetic Survey (NGS) cards¹⁰ that are used as input data for the analysis. Applying an equivalent sliding window median estimator, as used in Fig. 7, on the difference between the “Formal error for the observed delay” and “Modified formal error for the observed delay” provided in the NGS card produced the same annual signal as it can be seen in Fig. 7 (personal communication with Dr. Robert Heinkelmann, GFZ, Germany). The reason for the signal in the NGS card is still under investigation. For the combination process, this means that the annual signal, which was introduced for these two ACs by the different NGS lines, is compensated by the weighting factor and does not introduce a systematic

⁹ <http://vlbi.geo.tuwien.ac.at/>.

¹⁰ http://lacerta.gsfc.nasa.gov/mk5/help/dbngs_format.txt.

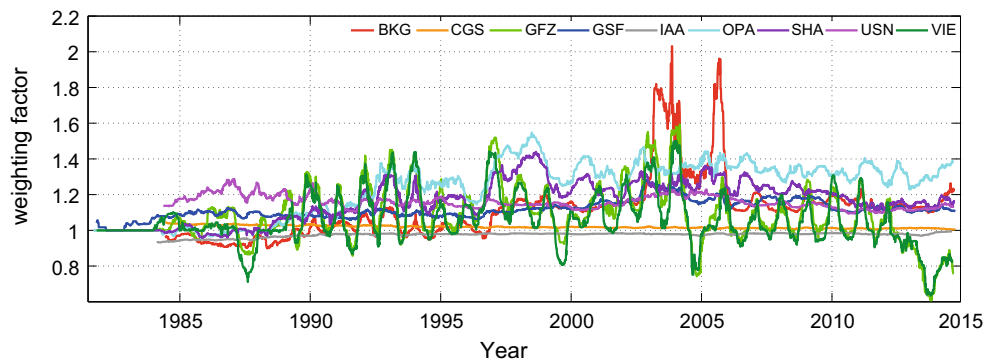


Fig. 7 Smoothed session-wise weighting factors of the individual ACs, using a sliding window of 90 days with 7 days moving median estimator

signal in the combined parameters, i.e. station coordinates and EOP.

3.3 VTRF combination strategy

Combined VLBI sessions contain all stations which participated in the IVS observing program, while only stations which are stable in their position and with a sufficient number of observed sessions are included in a terrestrial reference frame based on VLBI observations (VTRF). The VTRF is aligned with the ITRF so that the associated reference system of the VTRF is identical to the ITRS as it is described in the IERS Conventions (Petit and Luzum 2010, Chapter 4). This implies that the VTRF is a geocentric reference frame which is co-rotating with the Earth. Its origin is located in the center of mass of the Earth (geocenter, including oceans and atmosphere), the Z axis is the direction of the pole along the Earth's rotation axis, the orientation is equatorial with the X axis pointing towards the Greenwich meridian and the Y axis is orthogonal to the X and Z axis in a right handed system. The unit length is the SI-meter.

The VTRF is realized by a set of station positions and velocities at a given epoch, generated by the stacking of session-wise combined VLBI normal equations. The generation of a VTRF is based on the session-wise SINEX files of the combined solution resulting from the combination procedure described in Sect. 3.1.

Not all stations used for VLBI sessions are suitable to be integrated in the VTRF generations. The main criteria for integrating a VLBI station into the VTRF are the number of sessions in which the station participated and the time span where the observations have been carried out. Stations that have participated in less than ten sessions are excluded, as well as stations where all sessions have been observed within a short time span, e.g. 6 months. Some stations are affected by displacements resulting from earthquakes or man-made interventions. For these stations, multiple coordinates and velocities are estimated for the VTRF. The validity of each coordinate (and velocity) for stations with multiple epochs

is defined by a time stamp indicating the start and end time for the particular station. Data points of the piece-wise linear model for station coordinates and velocities are determined along the station coordinate time series by selecting points where significant changes in the direction are observed to best fit the station coordinate time series for all three coordinates. Generally, shorter intervals are chosen in the first years after the station displacement was observed (in case of earthquakes) since the post-seismic relaxation appears as higher order function. With decreasing magnitude of post-seismic relaxation, the order of the time series function decreases (first order function by approximation) and the time span between the data points of the piece-wise linear function are extended.

Figure 8 shows the combination strategy for a VTRF. The generation of a VTRF consists of two parts:

- Velocity estimation
- Accumulated TRF estimation.

For the velocity estimation EOPs and stations, that are deemed unsuitable for velocity estimation (e.g. due to too short observation time), are reduced from the normal equation in the session-wise combined SINEX files. Discontinuities are introduced for stations which underwent a telescope displacement (e.g. due to earthquakes). The a priori values for station coordinates are taken from the current ITRF. For new stations, stations with significant discontinuities, or stations that have not been introduced in the ITRF, a priori station coordinates are taken from the combined solution, and velocity a priori values are set to zero. Once the velocities are set up, the session-wise coordinates and velocities are accumulated. NNR and NNT conditions are applied for selected datum stations (cf. Fig. 2). For multiple telescopes that are built at the same site or telescopes that replace older ones on the same site, velocities are constrained on equal velocity values. Congruence/significance tests on those stations indicate whether station positions are stable enough to derive reliable velocities for these telescopes.

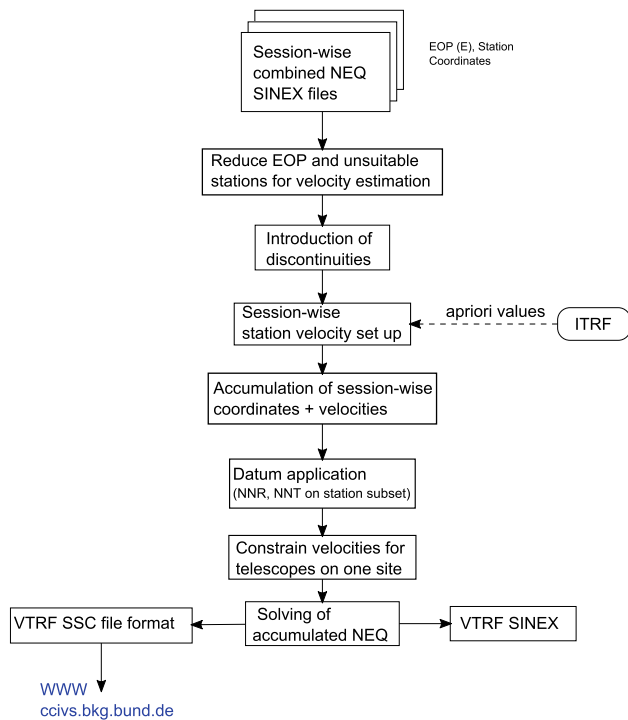


Fig. 8 Combination strategy for a TRF based on VLBI observations (VTRF)

The H_0 hypothesis established that both telescopes undergo the same velocity since they are built on the same tectonic area. The formula for the congruence test for an n -component test value (here $n = 3 = \{\dot{x}_{\text{North}}, \dot{x}_{\text{East}}, \dot{x}_{\text{Height}}\}$) with an error probability $\alpha = 0.001$ is given in Eq. (2). A congruence test gives the possibility to test if the velocities of the new telescope are accurate enough to be integrated into the VTRF.

$$T = \frac{\mathbf{d}^T \mathbf{Q}_{\mathbf{d}\mathbf{d}}^{-1} \mathbf{d}}{n} \sim F_{n, \infty, 1-\alpha} \mid H_0, \quad (2)$$

where $\mathbf{d} = \dot{\mathbf{x}}_2 - \dot{\mathbf{x}}_1$ and $\mathbf{Q}_{\mathbf{d}\mathbf{d}} = \mathbf{Q}_{\dot{\mathbf{x}}_1 \dot{\mathbf{x}}_1} + \mathbf{Q}_{\dot{\mathbf{x}}_2 \dot{\mathbf{x}}_2} - \mathbf{Q}_{\dot{\mathbf{x}}_1 \dot{\mathbf{x}}_2} - \mathbf{Q}_{\dot{\mathbf{x}}_2 \dot{\mathbf{x}}_1}$. $\dot{\mathbf{x}}_1$ and $\dot{\mathbf{x}}_2$ denote the velocities of station 1 and station 2, respectively, with the related variance-covariance matrix

$$\mathbf{Q}_{\dot{\mathbf{x}}_{1,2}} = \begin{bmatrix} \mathbf{Q}_{\dot{\mathbf{x}}_1 \dot{\mathbf{x}}_1} & \mathbf{Q}_{\dot{\mathbf{x}}_1 \dot{\mathbf{x}}_2} \\ \mathbf{Q}_{\dot{\mathbf{x}}_2 \dot{\mathbf{x}}_1} & \mathbf{Q}_{\dot{\mathbf{x}}_2 \dot{\mathbf{x}}_2} \end{bmatrix}.$$

Finally, T indicates if the H_0 hypothesis is accepted or must be rejected. The inversion of the accumulated normal equation leads to the final VTRF (SINEX and SSC format). Finally, the VTRF is published on the IVS Combination Center’s website.¹¹

¹¹ <http://ccivs.bkg.bund.de/>.

4 Station coordinate results

Station coordinates and EOP are the first results of the session-wise combination. While EOPs are a final product of the combination, station coordinates are building the basis for the determination of station velocities, annual signals in station height and a global solution in form of a TRF. In the following section, station coordinate and their follow-up results are presented. Results of the combined EOP are presented in Sect. 5.

Station coordinate results are generated by adding NNR and NNT conditions to the datum free combined normal equations of each session, and subsequently by inverting the normal equation matrix and solving for parameters.

4.1 Session-wise coordinates

Figure 9 shows station coordinate difference time series between the combined solution and the individual AC solutions for the north component of station Wettzell, Germany. In order to evaluate the station precision and repeatability, the WRMS of the session-wise time series of each station has been computed, as well as the overall WRMS for all stations. These statistical values give information about the quality of the contributions for every station. The WRMS is computed using Eq. (3), where \mathbf{x} denotes the vector of the combined results and \mathbf{x}_{AC} the vector of the individual results of the ACs with variance vector σ_0^2 .

$$\mathbf{p} = \frac{1}{\sigma_0^2}, \quad \mathbf{P} = \text{diag}(\mathbf{p})$$

$$\mathbf{v} = \mathbf{A}(\mathbf{A}^T \mathbf{P} \mathbf{A})^{-1} \mathbf{A}^T \mathbf{P} \mathbf{d} \mathbf{x} - \mathbf{d} \mathbf{x}$$

$$\mathbf{d} \mathbf{x} = \mathbf{x} - \mathbf{x}_{AC}, \quad \text{WRMS} = \sqrt{\frac{\mathbf{v}^T \mathbf{P} \mathbf{v}}{\text{trace}(\mathbf{P})}} \quad (3)$$

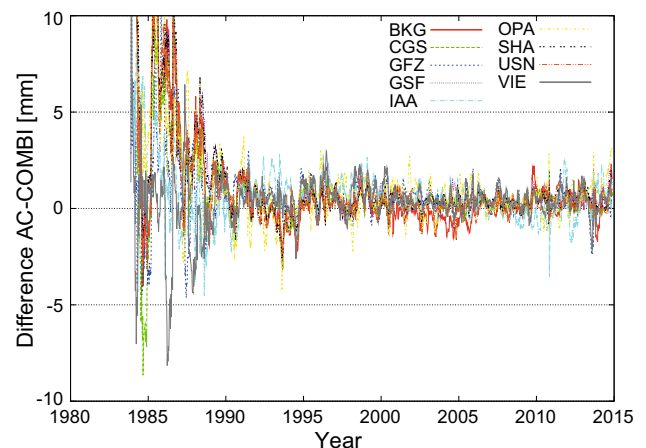


Fig. 9 Time series of north component differences between combined solution and individual solutions for station Wettzell, Germany

Table 3 gives an overview on the station participation and its repeatability (WRMS) for the combined solution. For simplicity, only stations with more than 30 successfully combined sessions are shown (cf. Fig. 3). The overall WRMS computed over the residuals of all stations (and all sessions) listed in Table 3 is 3.4 mm for north, 4.4 mm for east and 7.5 mm for height.

Figure 10 shows exemplarily the WRMS values from the session-wise time series for the north component of each AC and station. The east and height components show a similar situation concerning the quality and distribution—with a VLBI typical three times smaller height precision.

0.1, 0.25, 0.5, 0.75, 0.9 and 0.95 quantiles for combined station WRMS have been calculated using stations with more than 30 observed sessions, see Table 4. Ten percent of the stations (0.1 quantile) are better than 1.8 mm in north, 2.4 mm in east and 5.6 mm in height component. Fifty percent (0.5 quantile or median of station repeatability) are better than 4.4 mm in north, 5.8 mm in east and 9.3 mm in height component. Additionally, the table shows the minimum and maximum of station repeatability. The minimum is 1.5 mm in north component for stations BR-VLBA (Brewster, USA) and NL-VLBA (North Liberty, USA) (using 211 observed sessions each), 2.1 mm in east component for station ONSALA60 (Onsala, Sweden) (using 839 observed sessions) and 2.9 mm in height component for station HAYSTACK (Haystack, USA) (using 88 observed sessions). The maximum is 21.2 mm in north component for station MARPOINT (Maryland Point, USA) (using 76 observed sessions), 28.9 mm in east component for station SINTOTU3 (Kabato, Japan) (using 88 observed sessions) and 49.9 mm in height component for station OHIGGINS (O'Higgins, Antarctica) (using 127 observed sessions). These numbers have to be handled with care, because of the station's situation in Antarctica. Yearly observation epochs are performed on a regular basis, but they are short and limited to the Antarctic summer. The distribution of the measurements is thus not equally distributed over the year, which are suboptimal conditions for estimating station annual signals. Other stations in Table 3 have less observations than OHIGGINS, but the observations are equally distributed over the year leading to a better repeatability and a more reliable estimation of the station annual signal. Based on the repeatabilities in Table 3, the VGOS goal (accuracy of 1 mm and stability of 0.1 mm/year for global baselines, taken from Behrend et al. 2008) has not been reached yet.

The overall WRMS from the session-wise analysis for all stations shown in Fig. 10 for all ACs and the combined solution is summarized in Fig. 11 for north (red), east (green) and height (blue) component. The left part of the figure shows the WRMS for the ACs that were finally included into the combined solution (cf. Table 1). The WRMS values for the north component are between 3 and 4 mm and the east com-

Table 3 Overview on station participation and station repeatabilities WRMS for north (N), east (E) and height (H) component for the combined solution

Station ^a	Nb. Sess.	Ampl. (mm)	WRMS (mm)		
			N	E	H
AIRA	172	3.2 (1.7)	5.1	8.9	6.7
ALGOPARK	745	2.3 (0.6)	2.5	3.6	6.8
BADARY	293	4.5 (5.1)	3.8	7.9	17.2
BR-VLBA	211	4.1 (1.0)	1.5	2.7	5.0
CHICH10	160	0.9 (0.4)	6.1	9.4	6.0
CRIMEA	127	4.8 (2.8)	4.7	5.7	12.5
CTVASTJ	31	4.5 (1.1)	4.9	7.0	11.1
DSS15	101	4.6 (0.4)	4.4	8.8	7.3
DSS45	158	4.7 (2.4)	5.3	10.2	9.3
DSS65	119	3.5 (0.9)	2.4	3.1	4.0
EFLSBERG	42	4.9 (0.9)	1.9	2.3	8.9
FD-VLBA	258	0.9 (0.7)	1.8	2.3	4.8
FORTLEZA	1493	3.1 (1.6)	5.7	5.6	12.5
GGAO7108	76	16.6 (0.5)	3.0	4.5	12.7
GILCREEK	2046	2.2 (1.8)	3.3	8.1	5.7
HART15M	128	2.1 (2.1)	4.1	4.6	8.5
HARTRAO	1094	1.9 (2.1)	7.3	5.7	12.1
HATCREEK	181	2.5 (0.5)	6.0	8.7	12.5
HAYSTACK	88	6.4 (0.8)	1.8	3.5	2.9
HN-VLBA	200	2.1 (0.8)	2.0	2.3	6.4
HOBART12	359	6.9 (1.6)	7.5	11.0	12.5
HOBART26	811	2.4 (1.6)	7.0	13.7	13.9
HRAS_085	739	1.3 (0.7)	7.0	8.3	10.3
KASHIM11	45	9.7 (1.2)	8.2	27.1	16.6
KASHIM34	186	3.5 (1.2)	8.3	18.1	13.2
KASHIMA	264	4.1 (1.2)	5.6	11.4	9.5
KATH12M	270	2.9 (2.7)	5.1	4.5	11.6
KAUAI	485	0.8 (1.0)	4.3	8.1	6.4
KOGANEI	40	11.3 (1.4)	8.8	23.5	16.5
KOKEE	2091	1.2 (1.0)	5.3	6.3	9.1
KP-VLBA	196	1.9 (0.3)	1.7	2.5	4.3
LA-VLBA	263	1.9 (1.3)	1.6	2.4	5.5
MARPOINT	76	9.9 (0.5)	21.2	16.0	21.2
MATERA	911	3.3 (1.7)	3.4	2.9	7.9
MEDICINA	462	1.8 (1.4)	2.6	2.3	7.1
METSAHOV	63	4.5 (1.1)	3.3	2.9	9.6
MK-VLBA	209	1.4 (1.0)	2.5	3.8	5.8
MOJAVE12	735	1.5 (0.3)	3.8	6.1	5.7
MON_PEAK	38	9.2 (0.3)	7.3	8.3	15.0
NL-VLBA	211	1.1 (0.4)	1.5	2.3	5.5
NOTO	354	1.1 (1.5)	3.8	2.9	8.2
NRAO20	327	4.3 (0.5)	2.6	3.0	8.3
NYALES20	1526	1.7 (0.2)	2.4	2.2	6.8
OHIGGINS	127	246.4 (0.6)	8.6	8.4	49.9
ONSALA60	839	1.7 (0.6)	3.2	2.1	6.3

Table 3 continued

Station ^a	Nb. Sess.	Ampl. (mm)	WRMS (mm)		
			N	E	H
OVRO_130	202	6.2 (0.6)	1.6	2.6	6.1
OV-VLBA	128	0.8 (0.6)	5.3	9.8	14.6
PARKES	51	46.5 (2.9)	12.0	20.1	43.8
PIETOWN	252	0.7 (1.1)	2.6	3.9	7.7
RICHMOND	772	0.4 (0.7)	4.8	5.8	9.4
SANTOA12	128	4.3 (1.4)	9.3	8.3	17.3
SC-VLBA	206	0.6 (1.2)	2.7	3.3	6.9
SESHAN25	294	6.3 (3.7)	6.5	11.3	19.0
SINTOTU3	88	4.4 (1.4)	13.1	28.9	6.4
SVETLOE	473	2.2 (1.4)	2.7	3.6	10.4
SYOWA	66	28.0 (1.2)	8.9	13.8	24.6
TIGOCONC	1240	0.6 (1.2)	8.6	9.0	20.1
TSUKUB32	824	5.9 (1.3)	4.6	11.0	8.0
URUMQI	125	4.7 (5.5)	7.4	9.6	12.2
VERAISGK	52	5.1 (1.4)	7.0	6.2	12.5
VERAMZSW	81	3.8 (1.4)	7.9	27.6	19.3
VNDNBERG	181	4.4 (0.7)	5.1	7.0	15.7
WARK12M	110	11.8 (1.2)	5.6	11.8	15.6
WESTFORD	2296	0.9 (0.8)	3.0	3.6	6.1
WETTZELL	3232	1.9 (1.3)	3.1	2.6	6.6
NRAO85_3	1740	4.1 (0.5)	3.6	4.3	8.3
YARRA12M	253	1.9 (2.5)	3.9	5.7	10.5
YEBES40M	36	8.2 (0.9)	4.9	3.1	11.8
YEBES	178	2.7 (0.9)	1.8	2.8	6.0
YLOW7296	96	3.3 (1.3)	3.2	7.0	6.5
ZELENCHK	410	2.4 (3.5)	3.8	3.7	10.7

Only stations with more than 30 successfully combined sessions are listed. The annual amplitude is shown in mm. The annual amplitude of the corresponding Vienna NTAL model is shown in parentheses

^a IVS station names are indicated following <ftp://ivs.bkg.bund.de/pub/vlbi/ivscontrol/ns-codes.txt>

ponent between 4 and 6 mm, while the height component is about 7–9 mm—this is technique limited, due to imperfect observing networks and tropospheric mismodeling. The right part of the figure shows the combined solution result when AC AUS was included. The overall WRMS in this combined solution is noticeably increased, as in the final combined solution shown on the left side. Discrepancies in the implementation of meteorological parameters have meanwhile been identified to be the reason for the increased WRMS of station coordinates for AC AUS. In this situation, the decision was made by the IVS that a better combined solution was preferred to improving the heterogeneity of the AC contributions (i.e., including as many different software packages and analysis strategies as possible). Comparing the values of the combined solution with the values for the ACs,

the left part of Fig. 11 visualizes the underlying hypothesis of the combination: the combined solution is more accurate than the individual ACs (cf. Böckmann et al. 2010c), although the improvement is hardly visible. The WRMS for the combined solution is 3.3, 4.3, and 7.5 mm for north, east and height, while for the individual solutions the WRMS is between 3.4 and 4.5 mm, with a median of 3.6 mm) for north, 4.4 and 5.7 mm with a median of 4.7 mm for east, and between 7.7 and 9.2 mm with a median of 8.3 mm for the height component.

4.2 Annual signal in station height

Annual station signals are extracted from the station coordinate time series by cutting the time series into yearly segments and stacking the appropriate values of the height component. They show, among others, the monument movement of the telescope which is mainly influenced by atmospheric pressure loading and seasonal temperature variations and reflects the movement of the antenna over 1 year. It is, therefore, suitable to show the impact of the seasons along with the solar irradiation or precipitation at the telescope’s site. Periodic signals with periods longer than 1 year are not reflected in annual signals, but in the station time series.

Table 3 shows the amplitudes of the annual signal in mm. Before the computation of the amplitude, an outlier test of the station height time series was applied. The threshold for the outlier test is determined using the LMS method as described in Sect. 3.2.1. Here, the residuals contain the height component of the station coordinates.

Half of the stations have an annual amplitude of less than 3.3 mm and a semi-annual amplitude of less than 1.8 mm. 75 % of the stations show an annual amplitude of less than 4.8 mm and a semi-annual amplitude of less than 4.2 mm. For some stations with regular, but not continuous observations, such as OHIGGINS, which only observes within the same three months each year (i.e. December–February), a reliable annual amplitude cannot be estimated. Thus the results show unrealistic high values (crossed out value in Table 3).

Annual deformation signals of VLBI and GPS stations have been investigated, e.g. by Tesmer et al. (2009) using homogeneously reprocessed VLBI and GPS height time series. Comparing the characteristics for the mean annual station behavior for VLBI sites from Tesmer et al. (2009) with our results shows a good agreement (below 1 mm) with two example stations NYALES20 and WETTZELL (in Fig. 13). Other stations which have been analyzed by Tesmer et al. (2009) agree very well (within 1 mm) in terms of absolute amplitude, e.g. ALGOPARK, FORTLEZA, GILCREEK, KOKEE, ONSALA60 and TSUKUB32. Stations HARTRAO, HOBART26, MEDICINA and SESHAN25 agree within their formal uncertainty. Significant differences (3–4 mm) can be found, e.g. for station MATERA. Tesmer

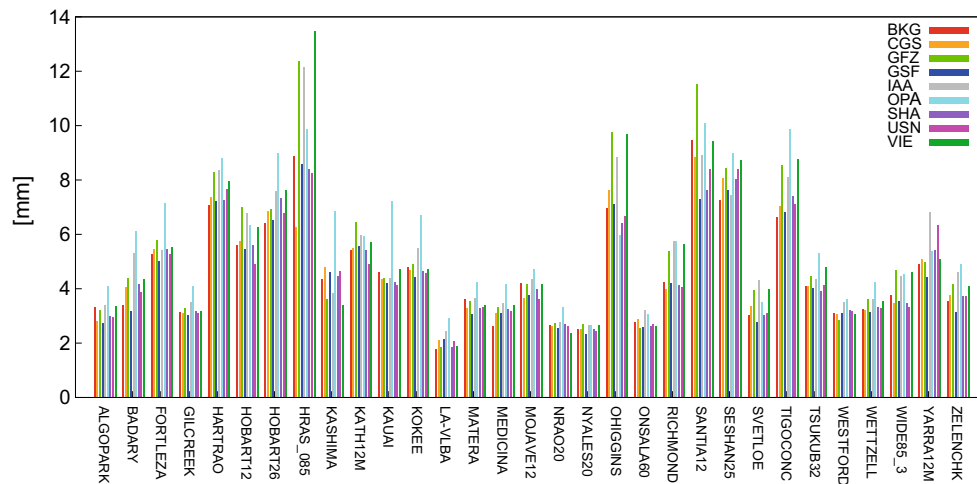


Fig. 10 WRMS of the session-wise analysis of the north component for all ACs and all stations which have been analyzed by all ACs and at least 30 successfully combined sessions

Table 4 Quantiles for combined station coordinates WRMS considering stations with more than 30 observed sessions

Quantile	North (mm)	East (mm)	Height (mm)
0.10	1.8	2.4	5.6
0.25	2.7	3.1	6.4
0.50	4.4	5.8	9.3
0.75	6.9	9.3	12.7
0.90	8.6	14.7	18.0
0.95	9.3	23.3	21.1
Minimum	1.5	2.1	2.9
Maximum	21.2	28.9	49.9

et al. (2009) considered observations done between 1994 and 2007. Station MATERA shows a larger data gap in its station coordinate time series between 2003 and 2005 and regular frequent observations afterward which can be an explanation for the differences found in the annual height amplitude.

One of the major geophysical effects expected to influence the station height variation is non-tidal atmospheric pressure loading (NTAL). The influence of NTAL is condensed in Fig. 12.

It shows the yearly amplitude of the height component (black squares) and the yearly amplitude resulting from the Vienna NTAL model¹² (red dots). The amplitudes were calculated by bi-linearly interpolating the gridded products (version 4). These grids have a 1° spatial resolution, and a temporal resolution of 6 h. The stations in Fig. 12 are sorted by the number of observed sessions in ascending order

from left to right. Stations with irregular observations are not shown (e.g. OHIGGINS). Both annual amplitudes are listed in Table 3 in the third column. Annual amplitudes resulting from the NTAL model are shown in parentheses. Not applying NTAL is one of the main differences between the combined IVS contribution to ITRF2014 and the operational rapid and quarterly combination provided by the IVS.¹³ Within the operational IVS combination, the ACs apply NTAL on the level of observations within the analysis.

Looking at Fig. 12 from left to right, the agreement between the amplitude of the yearly signal derived by VLBI observations and the amplitude resulting from the Vienna NTAL model improves with increasing number of sessions. Stations with relatively low amount of sessions (mainly in the first third of Fig. 12) show a larger disagreement than stations observing more sessions. These station time series are likely not yet suitable to determine a reliable annual signal. When considering stations that have more than one antenna, especially those where one antenna is considerably newer, this observation becomes clearer: the antenna with a longer observation time span generally agrees better than the newer antenna with a shorter observation time span, e.g. stations YEBES/YEBES40M (Yebes, Spain), KASHIM11/KASHIM34/KASHIMA (Kashima, Japan) and HOBART12/HOBART26 (Hobart, Tasmania, Australia). In contrast to this observation, the two telescopes at station HARTRAO/HART15M agree very well. Figure 13 shows the annual signal for stations NYALES20 (NyÅlesund, Svalbard, Norway) (top figure) and WETTZELL (Wetzell, Germany) (bottom figure) as well as the annual signal calculated from the Vienna NTAL model (black dashed line). The effect of

¹² Description and models: <http://ggsatm.hg.tuwien.ac.at/loading.html>.

¹³ <http://ccivs.bkg.bund.de/>.

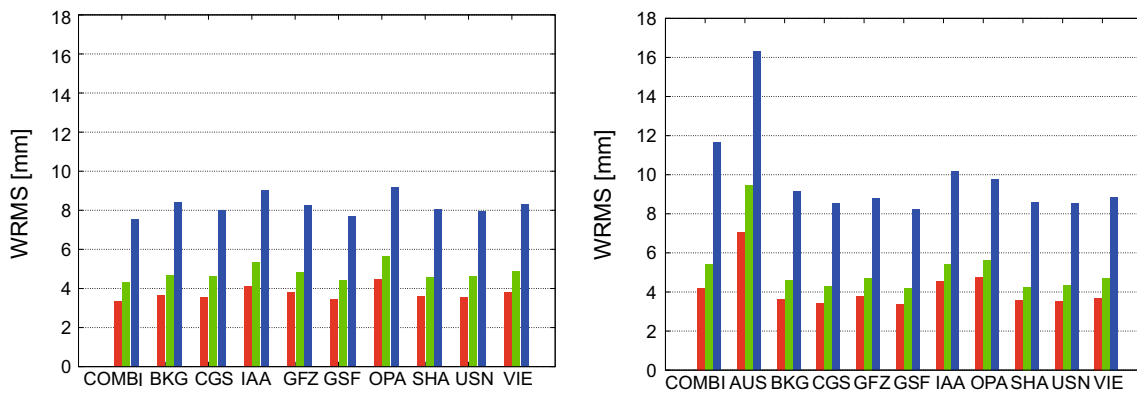


Fig. 11 WRMS of the session-wise analysis of north (red), east (green) and height (blue) of all stations for each AC and combined solution. The right part shows the results for a solution including AC AUS in

the combined solution, and the left part shows the solutions without the contribution of AC AUS

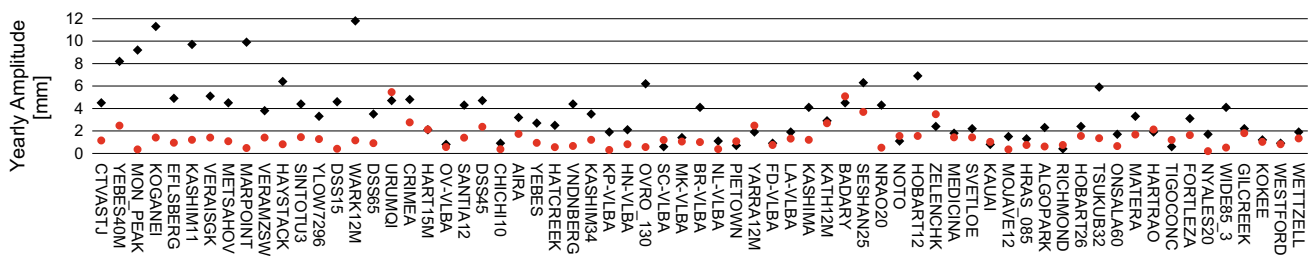


Fig. 12 Yearly amplitudes derived from VLBI observations (black squares) and determined by using the Vienna NTAL model (red dots). The stations are sorted by number of sessions in ascending order from left to right

NTAL is generally higher on stations that are situated in inland areas, such as WETTZEILL and lower for stations situated near the coastline, like NYALES20 (cf. Roggenbuck et al. 2015). This can be seen in Fig. 13, where the annual signal resulting from an NTAL is smoother for station NYALES20 than for station WETTZEILL, where the NTAL fits well with the annual signal resulting from VLBI observations, except for a small phase shift.

The influence on station height variation by applying atmospheric loading corrections a priori on the observation level (which is the case for operational IVS combination) or a posteriori on the estimated station coordinate has been studied, e.g. by Böhm et al. (2009). It was shown that the WMRS of the station height coordinate is not changing significantly by applying the a priori approach or the a posteriori approach. However, for small network sites of 4–6 stations (which is often the case for VLBI sessions, especially in the early years), neglecting atmospheric loading corrections at some stations propagates into the whole network through the application of NNR/NNT conditions. For some regions near enclosed seas or the Antarctica significant differences between the two approaches (a priori and a posteriori application of atmospheric loading) have been found by the authors. Based on these results the rigorous approach by applying

atmospheric loading corrections a priori on the observations level has been recommended.

For ITRF2014, removing periodic signals like annual and semi-annual signals from station time series, in place of NTAL, has been applied.¹⁴ The aim was to reduce the residuals (WRMS) of the station coordinate time series. Following this idea, 25 % of the stations show a yearly amplitude of more than 4.8 mm (cf. Table 3). Figure 12 shows that for newer telescopes and those telescopes with few observations or irregular participation in VLBI observations have a bad agreement with the amplitude of the annual signal taken from an NTAL model. However, a reliable annual amplitude can be derived from VLBI observations only for those stations with continuous observations over a longer time span.

Considering NTAL within the VLBI analysis also causes effects on other parameters than station coordinates. The impact of non-linear station motions on EOP and the celestial reference frame (CRF) has been investigated by Krásná et al. (2015). It has been shown that harmonic signals (e.g. annual signals) in station horizontal coordinates propagate directly into Earth rotation parameters X-Pole, Y-Pole and dUT1. Fur-

¹⁴ http://itrf.ign.fr/ITRF_solutions/2014/.

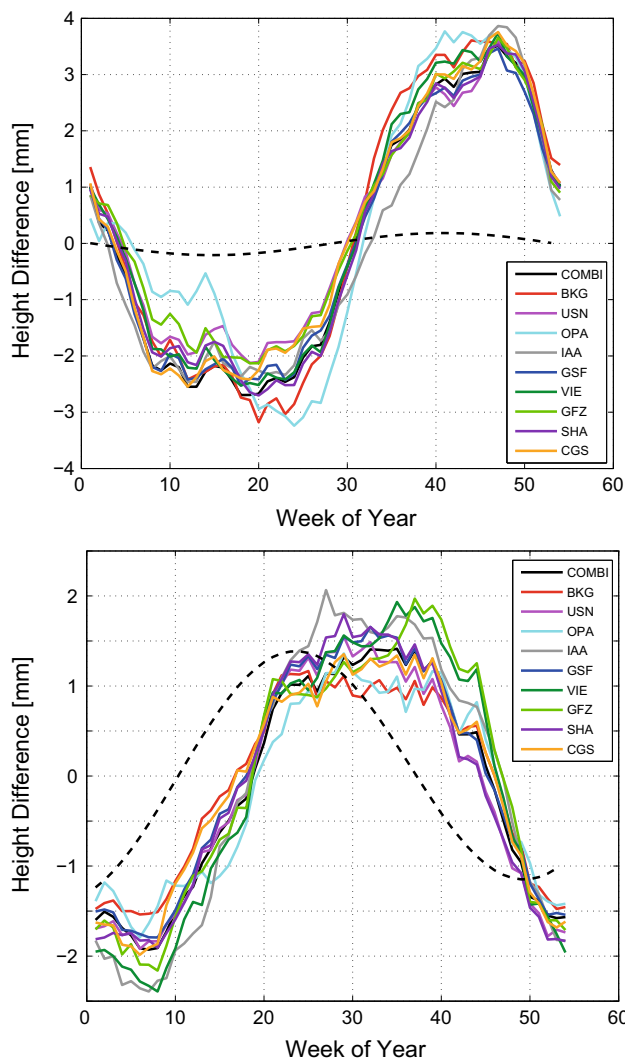


Fig. 13 Annual signals for stations NYALES20 (NyÅlesund, Svalbard, Norway) (*top figure*) and WETZELL (Wetzell, Germany) (*bottom figure*). The annual signal derived by the NTAL model is shown as *black dashed line*

thermore, seasonal station displacements can cause changes in radio source positions for sources with a low observation frequency and unevenly distributed observations. Applying seasonal model a priori to station coordinates to avoid distortive effects on ERF and CRF is recommended.

Other influences on the annual signal of the telescopes are continental water storage loading and non-tidal ocean loading, which can have a more significant influence than NTAL on some stations. The impact of the individual loading components on the station coordinates and other parameters is shown in Roggenbuck et al. (2015). Studying the influence of different loading models on VLBI stations goes beyond the scope of this paper. Further studies covering the influence of different loading models on the height variation of combined VLBI station results will follow.

4.3 VTRF

The VTRF generated following the description in Sect. 3.3 contains a set of station coordinates and velocities with a piece-wise linear model for each station and validity interval. The VTRF2014 is based on the IVS combined contribution to ITRF2014 with reference epoch 2005.0. Session-wise comparisons between the individual and the combined solutions as well as to the VTRF2014 solution are done for an internal validation of the scale. The VTRF2014 is then compared to DTRF2008 (Seitz et al. 2012) and ITRF2008 (Altamimi et al. 2011) for an external validation using a 14 parameter similarity transformation.

4.3.1 Internal validations for the scale

A session-by-session Helmert transformation is calculated between the combined solution and the individual solution, to compare the resulting scale parameters. The scale parameter of a transformation between two solutions of the same session (combined and individual) is independent of station displacement modeling (as used for a TRF generation) and is different from the scale relative to a TRF. Figure 14 shows the session-wise scaling factor between the combined and individual solutions, smoothed by a sliding median using a 90-day window and a 7-day moving step. Dates prior to 1994 are omitted for clarity reasons. Except for some local irregularities for some ACs, a good agreement between the individual AC solutions and the combined solution can be seen. The scale of the session-wise transformation is expected to be smaller than the scale compared to a TRF, where station displacements are introduced using a linear model.

A second internal validation is conducted between the individual scale parameter and the combined solution with respect to the global TRF solution VTRF2014. This comparison is shown in Fig. 15, where the scale factor is smoothed by a sliding median using a 90-day window and a 7-day moving step. The individual sessions are shown in gray. The annual signal of the scale parameter is shown in red calculated using the time span of ITRF2014 (i.e. 1979.6–2015.0) and in blue calculated using the time span of ITRF2008 (i.e. 1979.6–2009.0). A correlation between the scale parameter and the annual signal is clearly observable. Starting around the year 2010 the scale seems to have a reduced annual signal and higher frequency variations. Accordingly, a reduction of the amplitude may be expected if the whole ITRF2014 time span is used in contrast to the shorter time span of ITRF2008. Comparing the amplitudes of both annual signals a reduction of the amplitude of the red curve of about 0.01 ppb and a phase shift of 7 days can be observed (see detailed plot on the right top of Fig. 15). The variations starting in 2010 can thus be assumed as high-frequency noise covering the annual signal.

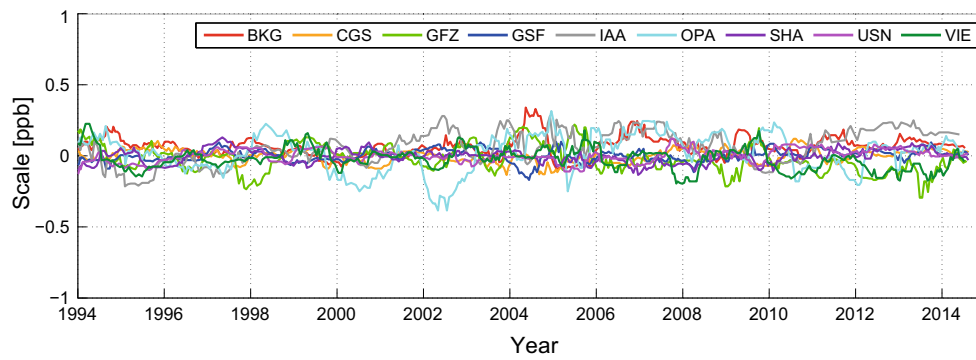


Fig. 14 Smoothed scale between combined and individual solution session-by-session since 1994. Data have been smoothed with a sliding median using a 90-day window and a 7-day moving step

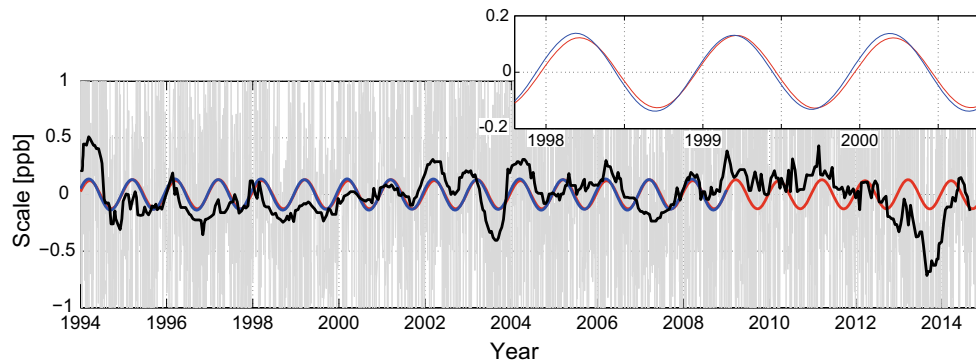


Fig. 15 Smoothed scale between VTRF2014 and session-wise combined solution since 1994 (*black*) and the annual signals calculated over the ITRF2014 time span (*red*) and over the ITRF2008 time span (*blue*).

Data have been smoothed with a sliding median using a 90-day window and a 7-day moving step. The *grey lines* connect the original data points

In contrast to Fig. 14, some clear irregularities can be seen: one in the end of 2003, and one towards the end of the data set before 2014. It is to be assumed that these irregularities are based on changes in the global station networks going along with unfavorable geometric station constellation. Additional investigation are presented in the following section. On close examination, a session-wise comparison is uncoupled from a reference frame so that it is independent of (linear) station modeling and residuals from the other station. The scale decrease before 2004 was already visible in Böckmann et al. (2010b) where the combined IVS contribution to ITRF2008 was compared to the ITRF2005. It seems likely that this irregularity is due to sessions with unfavorable station distribution. Between 2010 and 2012, many severe earthquakes have been registered within the IVS network. Additionally, several new epochs and discontinuities have been introduced into the VTRF2014, to get an adequate modeling of the station displacements. This has led to a more variable scale for these years, and the scale peculiarity towards the end of the data set is still unclear. It is possible that a situation similar to that in 2003 can be found with unfavorable station distribution. This aspect must be investigated when new

inter-technique combined TRFs (DTRF/ITRF) are available for scale comparisons.

4.3.2 External comparisons to DTRF and ITRF

Figure 16 shows the session-wise scale parameter of the combined solution with respect to DTRF2008, ITRF2008 and VTRF2014 for comparison reasons. In the first years of VLBI data acquisition (before 1994) the scale shows a more scattered behavior with an amplitude between -1 and $+1$ ppb for both comparisons (cf. red and blue curves in Fig. 16). The scatter of the scale flattens out in the following years, when the VLBI network contains more antennas and more sources are observed within one session. An offset of 0.3 ppb can be identified between the two comparisons starting around 1995. The mean offsets visible between the scale related to DTRF2008, ITRF2008 and VTRF2014 are consistent to the scale values presented in Tables 5 and 6. Starting in 2010, the VLBI network experienced significant antenna displacements due to several severe earthquakes in the Chilean and Japanese regions. These changes in the network, and the corresponding choice of datum stations for determining Helmert

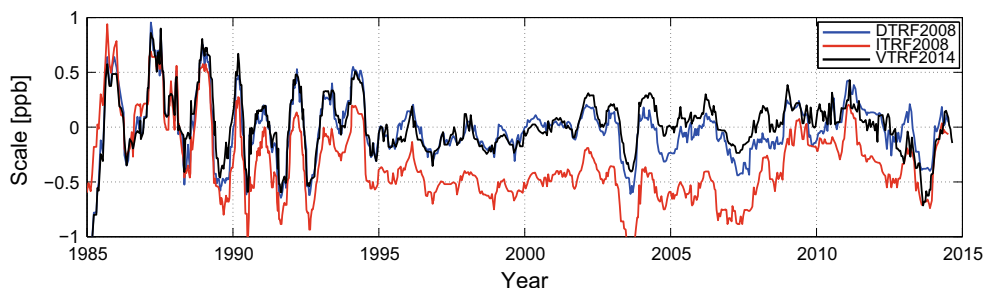


Fig. 16 Smoothed scale parameter between session-wise combined solution and DTRF2008 (blue) and with respect to ITRF2008 (red). For comparison reasons, the scale parameter with respect to VTRF2014 is shown in black

transformation parameters, are also visible in the evolution of the scale in both parts of Fig. 16.

The plot shows the same two peculiarities around 2004 and towards the end of the observations in 2014 as in Fig. 15. In the years around 2003/2004, the scale parameter suddenly seems to decrease to -0.6 ppb. Inspecting the sessions included in these two striking years, no particular antenna can be identified to introduce this effect (e.g. that of a displacement or a replacement). Comparing Fig. 10 in Böckmann et al. (2010b, p. 216) to Figs. 15 and 16, the same asymmetry in the mentioned period can be seen. The corresponding period contains many regional sessions with an unfavorable global station distribution for scale determination. A closer look at the scale parameters for this time period using only R1 or R4 sessions is provided in Fig. 17. The dashed line shows the scale containing only R1 sessions and the circled line containing only R4 sessions while the solid line contains all sessions corresponding to the scale shown in Fig. 16. The regularly observed (i.e., once per week each) IVS R1 and R4 sessions contain a minimum number of well-distributed participating stations. A reduction of the peculiarities around 2003/2004 is observed for both R1 and R4 sessions. Additionally, investigations have been done on the scale parameter development and dependency on the number of stations

within the respective sessions in 2004. It can be observed that for a network with at least seven stations, the irregularity around 2004 disappears. But since sessions with more than seven stations are observed neither frequently nor regularly, the observed scale smoothing effect should be handled with care. This observation corresponds to the assumption made before: the sessions around 2004 seem to be dominated by regional and small networks. An impact on the regional level seems to be caused by natural effects such as flood or drought, which are a possible explanation for the visible scale irregularities. Especially 2003 was a year of exceptional drought in the Northern hemisphere. Investigations to quantify these impacts on the scale parameter have to be done in the future to consider them for the weighting model.

The second irregularity around 2014 is influenced by the fact that both reference frames (DTRF2008 and ITRF2008) contain data only until the end of 2008. For sessions observed beyond this period, station coordinates must be extrapolated for several years. Furthermore, the VLBI network contains more new VLBI telescopes (see Fig. 3) which are not part of DTRF2008 and ITRF2008. This decreases the selection of datum stations for the Helmert transformation.

Tables 5 and 6 show transformation parameters of the VTRF2014 with respect to DTRF2008 and ITRF2008, as well as the RMS of the transformation residuals. In the tables, t_x, t_y and t_z denote the respective translation parameters, r_x, r_y and r_z the respective rotation parameters, and D denotes the scale parameter. For the comparisons, a 14-parameter Helmert transformation is calculated, including position and velocity of the TRF. The transformation between the VTRF-2014, DTRF2008 and ITRF2008 has been generated using 51 stations out of 158, which have demonstrated long-term stability. The estimated standard deviation of the transformation residuals (position and velocity) is 4.9 mm when compared to DTRF2008, and 3.5 mm when compared to ITRF2008. The RMS of transformed coordinate and velocity residuals is 4.8 mm and 0.9 mm/year, respectively, for DTRF2008 and 3.5 mm and 0.8 mm/year, respectively, for ITRF2008. The rotation angles r_x, r_y , and r_z , as well as the translations t_x, t_y and t_z are, as expected to be, very small

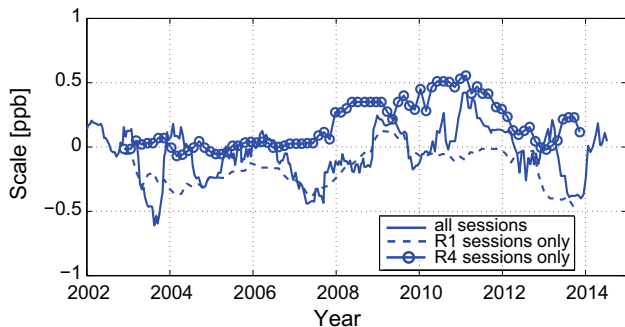


Fig. 17 Detailed view of the smoothed scale parameter between session-wise combined solution and DTRF2008 (solid line, agreeing with Fig. 16), when only R1 (dashed line) and when only R4 sessions are used (circled line)

Table 5 Transformation parameters between VTRF2014 and DTRF2008 (Epoch 2005.0)

Name	t_x (mm)	t_y (mm)	t_z (mm)	D (ppb)	r_x (mas)	r_y (mas)	r_z (mas)
Position	-2.1	-0.1	1.1	0.11 (0.7)	-0.03 (-1.0)	0.06 (1.7)	-0.12 (-3.5)
σ_{Pos}	0.8	0.8	0.7	0.11	0.03	0.03	0.03
Velocity	t_x (mm/year)	t_y (mm/year)	t_z (mm/year)	D (ppb/year)	r_x (mas/year)	r_y (mas/year)	r_z (mas/year)
	-0.5	-0.6	0.2	0.02 (0.1)	-0.006 (-0.2)	0.002 (0.1)	0.006 (0.2)
$\sigma_{Velocity}$	0.8	0.8	0.7	0.11	0.03	0.03	0.03

The values in parentheses denote the equivalent on the Earth's surface in mm

Table 6 Transformation parameters between VTRF2014 and ITRF2008 (Epoch 2005.0)

Name	t_x (mm)	t_y (mm)	t_z (mm)	D (ppb)	r_x (mas)	r_y (mas)	r_z (mas)
Position	-0.8	0.6	-1.1	0.44 (2.8)	-0.02 (-0.6)	-0.01(-0.3)	0.01 (0.3)
σ_{Pos}	0.6	0.6	0.6	0.09	0.02	0.02	0.02
Velocity	t_x (mm/year)	t_y (mm/year)	t_z (mm/year)	D (ppb/year)	r_x (mas/year)	r_y (mas/year)	r_z (mas/year)
	-0.4	-0.4	0.1	-0.02 (-0.1)	-0.008 (-0.2)	0.006 (0.2)	0.012 (0.4)
$\sigma_{Velocity}$	0.6	0.6	0.6	0.09	0.02	0.02	0.02

The values in parentheses denote the equivalent on the Earth's surface in mm

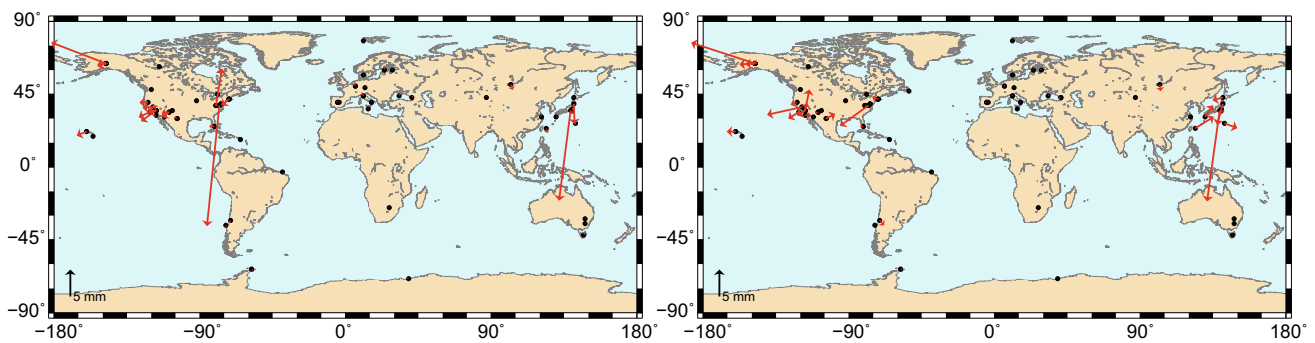


Fig. 18 Horizontal station coordinate residuals after Helmert transformation of VTRF2014 with respect to DTRF2008 (left) and ITRF2008 (right). Only stations with more than 30 successfully combined sessions are shown

due to NNR and NNT conditions applied on the datum stations to keep the frames consistent. Only the scale parameter is directly accessible by VLBI. Here, the two comparisons show noticeable differences: the scale difference with respect to ITRF2008 is 0.44 ppb and with respect to DTRF2008 is 0.11 ppb.

Figure 18 shows the horizontal station coordinates residuals with respect to DTRF2008 (left) and ITRF2008 (right). Only stations with more than 30 observations are shown since only stations with a certain number of observations can be determined precisely enough. Stations with residuals bigger than 10 mm are KOGANEI (Koganei, Japan) and GILCREEK (Gilmore Creek, Alaska, USA west coast, 2nd epoch only, corresponding to coseismic offset in November 2002) for both comparisons, with MARPOINT (Maryland Point, USA east coast) for DTRF2008 only. Combining the north and east residual to one horizontal component, 10 % of the residuals are below 0.12/0.12 cm, 25 % are below

0.19/0.14 cm, 50 % are below 0.32/0.24 cm, 90 % are below 1.98/2.74 cm and 95 % are below 5.68/5.15 cm. The first number indicates the values with respect to DTRF2008, and the second the values with respect to ITRF2008 (cf. Fig. 18). For the height residuals of both comparisons, 10 % of the residuals are below 0.05/0.06 cm, 25 % are below 0.15/0.17 cm, 50 % are below 0.40/0.42 cm, 90 % are below 2.91/3.09 cm and 95 % are below 9.76/8.61 cm (cf. Fig. 19).

When considering the large differences of the two scale offsets among VTRF2014, DTRF2008 and ITRF2008, larger differences in the station residuals are expected. Comparing the two residual groups, the differences with respect to DTRF2008 and ITRF2008 are within the sub-cm range without significant differences. The differences between the scale offsets between the VTRF2014 and inter-technique combined TRFs (DTRF, ITRF and other inter-technique TRF realizations), including the impact on station residuals in horizontal and vertical components, have to be studied in further

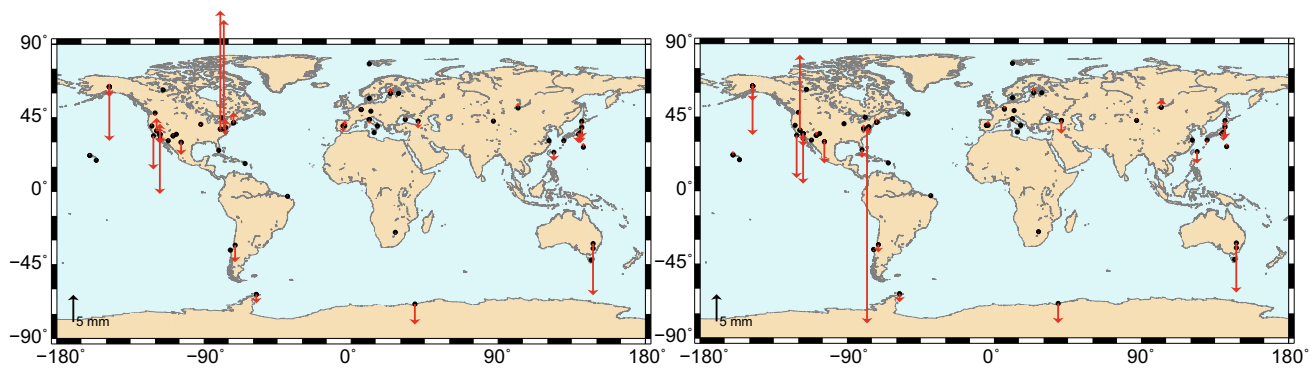


Fig. 19 Height station coordinate residuals after Helmert transformation of VTRF2014 with respect to DTRF2008 (*left*) and ITRF2008 (*right*). Only stations with more than 30 successfully combined sessions are shown

Table 7 Offset and rate of the individual and combined solution with respect to different TRF and their standard deviation in parentheses

AC	DTRF2008		ITRF2008		VTRF2014		COMBI	
	Off (ppb)	Rate ppb/year	Off (ppb)	Rate ppb/year	Off (ppb)	Rate ppb/year	Off (ppb)	Rate ppb/year
COMBI	-0.14	0.01	-0.50	0.00	-0.06	0.01	—	—
BKG	-0.14	0.03	-0.48	0.02	-0.07	0.02	0.05	0.00
CGS	-0.10	0.05	-0.25	-0.03	0.04	0.00	0.04	-0.01
GFZ	-0.09	0.00	-0.42	0.01	-0.04	-0.01	-0.08	0.00
GSFC	-0.10	0.02	-0.42	0.00	0.14	-0.02	-0.02	0.00
IAA	-0.12	0.02	-0.51	0.01	0.37	-0.06	0.00	0.01
OPAR	-0.07	-0.03	-0.38	-0.03	0.08	-0.01	0.10	-0.01
SHAO	-0.09	0.00	-0.47	-0.00	0.07	-0.01	0.01	0.00
USNO	-0.12	0.00	-0.41	-0.01	0.01	0.00	0.01	0.00
VIE	-0.12	0.00	-0.49	-0.01	-0.06	0.01	-0.05	0.00

detail once the various ITRS realizations covering the same time span as the VTRF2014 are published.

4.3.3 VTRF summary

Table 7 summarizes offset and rate of the scale time series between the session-wise solutions (individual ACs and IVS combination) and the various TRF solutions (DTRF, ITRF) which have been shown in the previous section. Comparing the offset of the session-wise solutions (individual AC and combined) with respect to DTRF2008, variations between -0.07 and -0.14 ± 0.02 ppb are visible. Compared to the ITRF2008, the offset values of the scale vary between -0.25 and -0.51 ± 0.02 ppb. The overall offset of the scale parameter between the session-wise solutions (individual and combined) and the DTRF2008 is about 0.3 ppb (corresponding to 1.9 mm on the Earth's surface) smaller than the overall scale offset with respect to ITRF2008 (with equal standard deviations). This value agrees with the scale differences compared to Tables 5 and 6. The reason for the differences in the scale parameter could reside in the different use of local tie surveys and in different ways of averaging the SLR

and VLBI scales in the inter-technique combination process implemented for DTRF2008 and ITRF2008. Examining the scale rates, the differences between the comparisons with respect to DTRF2008 and ITRF2008 are not as large as for the offset parameter. For DTRF2008 the rates vary between -0.03 and 0.05 ± 0.002 ppb/year and for ITRF2008 between -0.03 and 0.02 ± 0.003 ppb/year.

A different case is the comparison of the individual and combined solutions with respect to VTRF2014. The scale offsets and rates in columns 6 and 7 of Table 7 are about one order of magnitude smaller than compared to DTRF2008 and ITRF2008. This is due to the input data used for calculating the TRFs. The scale offset is between -0.07 and 0.14 ± 0.02 ppb, except for IAA AC, where the scale is 0.37 ppb. The reason for the elevated scale offset for this AC is not yet clear. The rate of the individual ACs and combined solution with respect to VTRF2014 is between -0.01 and 0.06 ± 0.002 ppb/year.

While data of all four geodetic space techniques are used (cf. Seitz et al. 2012; Altamimi et al. 2011) for DTRF2008 and ITRF2008, the VTRF2014 is only based on VLBI observations and thus has a smaller offset and rate when compared

to the external TRFs. Furthermore, the VTRF2014 contains data until the end of 2014—six more years of data than DTRF2008 and ITRF2008. The last two columns show the scale based on a VLBI internal session-wise comparison between the combined solution and the individual solutions (i.e. no TRF is used). Here, the scale offset is -0.08 to 0.1 ± 0.008 ppb and the scale rate is -0.01 to 0.0 ± 0.001 ppb/year. The smoothed scale time series corresponding to the offsets is shown in Fig. 14.

5 EOP results

EOPs are the second parameter type besides station coordinates resulting directly from the combination. The EOPs contain pole coordinates (*X*- and *Y*-pole) and rates, UT1-UTC (dUT1), and the rate Length of Day (LOD) and nutation parameters *dX* and *dY*. VLBI is the only geodetic space technique providing a full set of EOP, including a link to the celestial reference frame. EOPs are estimated by fixing datum station coordinates on their a priori values within 0.001 mm, which makes it critical to carefully select station a priori values and datum stations. In the following section, the results of the combined EOP are presented, making use of internal comparisons as well as external comparisons to C04 series (Bizouard and Gambis 2010).

For the first time, all parameters of the combined normal equations are transformed to 12 h UT to be consistent with the other geodetic space techniques (cf. Sect. 4). IVS 24-h sessions are usually scheduled between 17:00 UT and 17:00

UT of the following day. EOP and station positions determined at 12 h UT are shifted by about 7 h compared to the routine IVS combination where all parameters are estimated at mid-session.

5.1 Internal consistency

Figures 20 and 21 show the smoothed time series of the differences between the individual AC solutions and the combined solution for dUT1 and *X*-Pole, which are shown as examples for all EOPs. Similar to the station coordinates, the first years of VLBI data collection were still very scattered until VLBI observations accuracy increased in the early 1990s. The median differences between the individual AC solution and the combined solution vary between -10 and $10 \mu\text{s}$ for dUT1 and between -50 and $50 \mu\text{as}$ for *X*-Pole (leaving out the years before 1994) including some peaks.

Figures 22 and 23 show the WRMS of the differences between the individual solutions and the combined solution for *X*- and *Y*-Pole (bars) and their rates (lines) and for dUT1 (bars) and LOD (lines). Only sessions which have been analyzed successfully by all ACs have been used for the comparisons.

The WRMS is between 40 and 100 μas for *X*-Pole and *Y*-Pole and between 5 and 15 μs for dUT1. Since VIE AC provided piecewise linear offsets for all EOPs, instead of offset and rate, a transformation to offset and rate was included a priori to the combination process, which seems to be not as accurate as if the parameterization is directly introduced within the analysis process. The WRMS for *X*- and *Y*-Pole

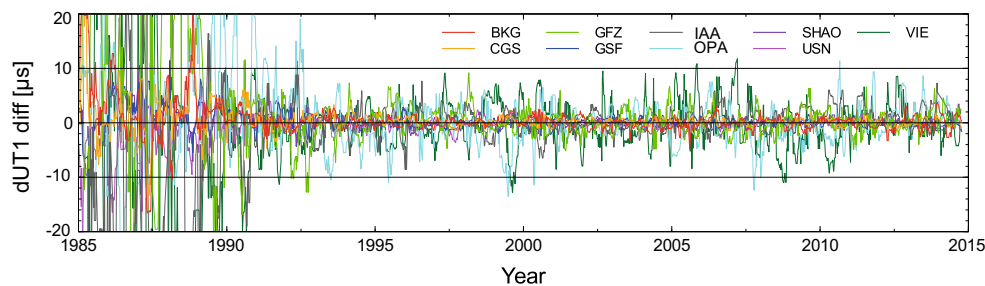


Fig. 20 dUT1 differences between individual and combined solution smoothed with a 70-day moving median filter

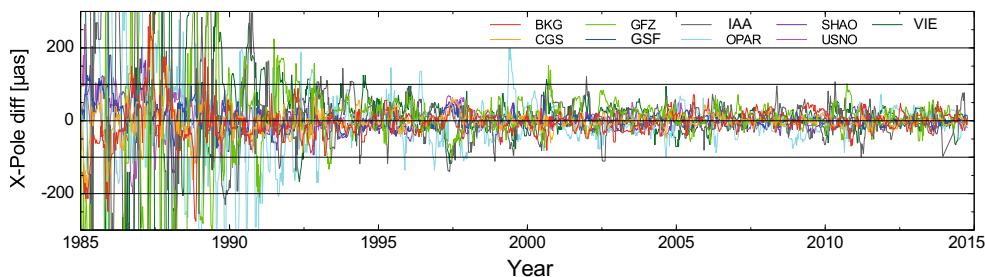


Fig. 21 *X*-Pole differences between individual and combined solution smoothed with a 70-day moving median filter

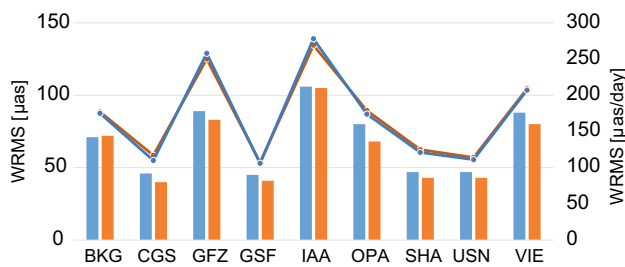


Fig. 22 WRMS of the differences between the individual and combined solution for X - and Y -pole (bars) and their rates (lines)

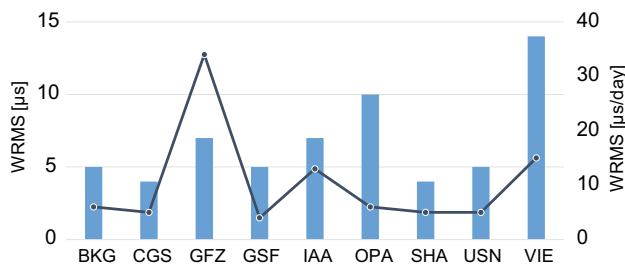


Fig. 23 WRMS of the differences between the individual and combined solution for dUT1 (bars) and LOD (lines)

rates are between 100 and 250 $\mu\text{s/day}$ and for LOD between 5 and 15 $\mu\text{s/day}$. Further studies are required to find the reason for the increased LOD WRMS found for GFZ AC. The WRMS for the nutation parameter (not shown) are between 30 and 80 μs for dX and dY . An elevated WRMS for nutation can be found for AC OPA with $\sim 140 \mu\text{s}$. The reason for the increased nutation differences for OPA AC is still open to investigation.

5.2 External consistency with IERS-08-C04

For an external comparison, the combined EOP results are compared to the IERS C04 series (cf. Bizouard and Gambis 2010). Table 8 summarizes the WRMS of the combined EOP parameter with respect to C04 series. X - and Y -Poles show an average WRMS difference of 138 μs and an aver-

Table 8 WRMS values for the difference between the combined EOP solution and IERS C04 series

EOP	COMBI
X -Pole (μs)	132
Y -Pole (μs)	143
X -Pole rate ($\mu\text{s/day}$)	482
Y -Pole rate ($\mu\text{s/day}$)	454
dUT1 (μs)	13
LOD ($\mu\text{s/day}$)	39
dX (μs)	63
dY (μs)	67

age WRMS difference for their rates of 468 $\mu\text{s/day}$. The WRMS for dUT1 is 13 μs and 39 $\mu\text{s/day}$ for LOD. For the nutation parameters dX and dY , the average WRMS difference is 65 μs . These values are of the same magnitude as found in Vennebusch et al. (2007). The values for dUT1 and the nutation parameters of the IERS C04 series are derived from VLBI observations only. Thus, these values cannot be treated as completely independent, in contrast to the pole parameters and LOD which are a combined product of different space geodetic techniques.

6 Summary and conclusion

The IVS submitted 5796 combined 24-h sessions for the ITRF2014 contribution, covering a time span from 1979 to the end of 2014. Eleven IVS Analysis Centers using five different software packages submitted contributions to the combined solution. After a careful selection process, nine contributions using three different software packages were included in the combined solution. The combined solution contains 158 stations. Compared to the IVS contribution to the ITRF2008, an improved outlier test and weighting strategy was implemented. The station repeatability over all stations (WRMS) is 3–4 mm for the horizontal components (north and east) and 8–9 mm for the height component for all included Analysis Centers. 75 % of the stations have a repeatability of better than 6.9 mm for north, 9.3 mm for east and 12.7 mm for height component. Within the last years the VLBI network expanded in size and in quality. It can be expected that this will also have a positive impact on the station coordinate quality within the upcoming years. Improving the session weighting by considering the geometric network characteristics for global VTRF solutions is one of the next steps.

An increasing agreement can be observed between the annual station signals of stations with a longer time span and the annual amplitude derived from an NTAL model. For stations with few or irregular observations, the reliable determination of the annual signal remains difficult. The differences between the annual signal derived from VLBI station coordinates and from the NTAL model are noticeably higher for these stations.

VLBI and SLR are the only space geodetic techniques providing the scale parameter to the ITRF2014. Comparing the combined solution to different TRF solutions shows significant differences in the trend and magnitude of the scale. Comparisons to the ITRF2008 show a scale offset of 0.44 ppb, while comparisons to the DTRF2008 show a scale offset of only 0.11 ppb. The choice of datum stations also has a significant impact on the scale parameter, but the choice is limited because of the relatively small VLBI networks. Upcoming developments in the frame of VGOS will provide

the opportunity to make further investigations on the VLBI scale parameter.

EOP comparisons show generally a good agreement between the individual contributions and the combined solution. The WRMS of the differences are between 40 and 100 μs for X - and Y -Pole, between 5 and 15 μs for dUT1, and between 5 and 35 $\mu\text{s/day}$ for LOD. Further investigations must be done to find the reason for the increased differences for dUT1 and LOD for the VieVS and VieVS@GFZ solutions.

Acknowledgments The VLBI intra-technique combination is the last link of a process chain starting with the planning and realization of the VLBI observations. We want to thank everyone who contributes to this process, especially the IVS Analysis Centers who provided the input data for the combination process. Furthermore, we want to thank the responsible persons at the IERS ITRS Combination Centers at DGFITUM, IGN, and JPL who provided valuable remarks on the combined sessions. The support by the DFG research unit FOR 1503 for the studies on atmospheric loading is acknowledged, too. Finally, we want to thank R. Bertelmann, R. Heinkelmann and A. Nothnagel for the work on introducing the data DOI for the VTRF, to pay tribute to all contributors and to provide a reference for the wealth of VLBI data used in the VTRF combination.

References

- Altamimi Z, Collilieux X, Métivier L (2011) ITRF2008: an improved solution of the international terrestrial reference frame. *J Geod* 85(8):457–473. doi:10.1007/s00190-011-0444-4
- Bachmann S, Lösler M (2012) IVS combination center at BKG—robust outlier detection and weighting strategies. In: Behrend D, Baver K (eds) IVS 2012 general meeting proceedings, NASA/CP-2012-217504, pp 261–265
- Behrend D, Böhm J, Charlot P, Clark T, Corey B, Gipson J, Haas R, Koyama Y, MacMillan D, Malkin Z, Niell A, Nilsson T, Petraschenko B, Rogers A, Tuccari G, Wresnik J (2008) Recent progress in the VLBI2010 development. In: Sideris MG (ed) Observing our changing Earth, international association of geodesy symposia, vol 133, Springer, Heidelberg, pp 833–840. doi:10.1007/978-3-540-85426-5_96
- Bizouard C, Gambis D (2010) The combined solution C04 for Earth orientation parameters consistent with international terrestrial reference frame 2008. In: Technical report, IERS Earth Orientation Product Centre. http://hpiers.obspm.fr/iers/eop/eopc04/C04_guide
- Böckmann S, Artz T, Nothnagel A (2010) Correlations between the contribution of individual IVS analysis centers. In: Behrend D, Baver KD (eds) IVS 2010 general meeting proceedings, NASA/CP-2010-215864, pp 222–226
- Böckmann S, Artz T, Nothnagel A (2010) VLBI terrestrial reference frame contributions to ITRF2008. *J Geod* 84(3):201–219. doi:10.1007/s00190-009-0357-7
- Böckmann S, Artz T, Nothnagel A, Tesmer V (2010) International VLBI service for geodesy and astrometry: Earth orientation parameter combination methodology and quality of the combined products. *J Geophys Res* 115(B04404). doi:10.1029/2009JB006465
- Böhm J, Werl B, Schuh H (2006) Troposphere mapping functions for GPS and very long baseline interferometry from European Centre for Medium-Range Weather Forecasts operational analysis data. *J Geophys Res* 111(B02406). doi:10.1029/2005JB003629
- Böhm J, Heinkelmann R, Mendes Cerveira PJ, Pany A, Schuh H (2009) Atmospheric loading corrections at the observation level in VLBI analysis. *J Geod* 83(11):1107–1113. doi:10.1007/s00190-009-0329-y
- Böhm J, Böhm S, Nilsson T, Pany A, Plank L, Spicakova H, Teke K, Schuh H (2012) Geodesy for planet Earth—the new Vienna VLBI software VieVS. International association of geodesy symposia, vol 136, chap 7. Springer, Berlin, pp 1007–1011. doi:10.1007/978-3-642-20338-1
- Chen G, Herring TA (1997) Effects of atmospheric azimuthal asymmetry on the analysis of space geodetic data. *J Geophys Res* 102(B9):20489–20502. doi:10.1029/97JB01739
- Davis JL, Herring T, Shapiro II, Rogers AEE, Elgered G (1985) Geodesy by radio interferometry: effects of atmospheric modeling errors on estimates of baseline length. *Radio Sci* 20(6):1593–1607
- Egbert G, Bennett A, Foreman M (1994) TOPEX/POSEIDON tides estimated using a global inverse model. *J Geophys Res* 99(C12):24821–24852
- Fey AL, Gordon D, Jacobs CS (2009) The second realization of the international celestial reference frame by very long baseline interferometry (IERS technical note no. 35). Verlag des Bundesamtes für Kartographie und Geodäsie, Frankfurt am Main (ISBN 978-3-89888-918-6)
- Fey AL, Gordon D, Jacobs CS, Ma C, Gaume RA, Arias EF, Bianco G, Boboltz DA, Böckmann S, Bolotin S, Charlot P, Collioud A, Engelhardt G, Gipson J, Gontier AM, Heinkelmann R, Kurdubov S, Lambert S, Lytvyn S, MacMillan DS, Malkin Z, Nothnagel A, Ojha R, Skurikhina E, Sokolova J, Souchay J, Sovers OJ, Tesmer V, Titov O, Wang G, Zharov V (2015) The second realization of the international celestial reference frame by very long baseline interferometry. *Astron J* 150(2):58. doi:10.1088/0004-6256/150/2/58
- Förstner W (1979) Ein Verfahren zur Schätzung von Varianz- und Kovarianzkomponenten. *Allg Vermess Nachr* 11–12:446–453
- Heinkelmann R, Bertelmann R, Klump J, Schuh H (2013) Make it citable: data in IVS. In: 21st meeting of the European VLBI group for geodesy and astrometry (EVGA). http://evga.fgi.fi/sites/default/files/u3/s3_talk5_Heinkelmann_Make_it_citable
- Jäger R, Müller T, Saler H, Schwäble R (2005) Klassische und robuste Ausgleichungsverfahren. Herbert Wichmann-Verlag, Heidelberg. ISBN 978-3-87907-370-2
- Krásná H, Malkin Z, Böhm J (2015) Non-linear VLBI station motion and their impact on the celestial reference frame and Earth orientation parameters. *J Geod* 89(10):1019–1033. doi:10.1007/s00190-015-0830-4
- Kutterer H, Heinkelmann R, Tesmer V (2003) Robust outlier detection in VLBI data analysis. In: Schwegmann W, Thorand V (eds) Proceedings of the 16th EVGA working meeting. Verlag des Bundesamtes für Kartographie und Geodäsie, Leipzig/Frankfurt am Main, pp 247–256
- Lösler M (2011) Robust parameter estimation of the spatial Helmert transformation (in German). *Allg Vermess Nachr* 118(5):179–186
- Lyard F, Lefevre F, Letellier T, Franci O (2006) Modelling the global ocean tides: modern insights from FES2004. *Ocean Dyn* 56:394–415. doi:10.1007/s10236-006-0086-x
- MacMillan D (1995) Atmospheric gradients from very long baseline interferometry observations. *Geophys Res Lett* 22(9):1041–1044. doi:10.1029/95GL00887
- MacMillan DS, Ma C (1997) Atmospheric gradients and the VLBI terrestrial and celestial reference frames. *Geophys Res Lett* 24(4):453–456. doi:10.1029/97GL00143
- Mathews PM, Dehant V, Gipson J (1997) Tidal station displacements. *J Geophys Res* 102(B9):20469–20477. doi:10.1029/97JB01515
- McCarthy D, Petit G (2003) IERS conventions 2003. IERS technical note no. 32. Verlag des Bundesamtes für Kartographie und Geodäsie, Frankfurt am Main (ISBN 3-89888-884-3)

- Neitzel F (2003) Identifizierung konsistenter Datengruppen am Beispiel der Kongruenzuntersuchung geodätischer Netze. PhD thesis, Bayer. Akademie d. Wissenschaften (ISBN 978-3769650044)
- Nothnagel A (2009) Conventions on thermal expansion modelling of radio telescopes for geodetic and astrometric VLBI. *J Geod* 83:787–792. doi:[10.1007/s00190-008-0284-z](https://doi.org/10.1007/s00190-008-0284-z)
- Nothnagel A (2015) The IVS data input to ITRF2014. In: International VLBI service for geodesy and astrometry, GFZ data services. International VLBI service for geodesy and astrometry (IVS). doi:[10.5880/GFZ.1.1.2015.002](https://doi.org/10.5880/GFZ.1.1.2015.002)
- Petit G, Luzum B (2010) IERS conventions 2010. IERS technical note no. 36. Verlag des Bundesamtes für Kartographie und Geodäsie, Frankfurt am Main (ISBN 978-3-89888-989-6)
- Roggenbuck O, Thaller D, Engelhardt G, Mareyen M, Franke S, Dach RPS (2015) Loading-induced deformation due to atmosphere, ocean and hydrology: model comparisons and the impact on global SLR, VLBI and GNSS solutions. In: International association of geodesy symposia, vol 146, Springer, Berlin (in press). doi:[10.1007/1345_2015_214](https://doi.org/10.1007/1345_2015_214)
- Rousseeuw P (1984) Least median of squares regression. *J Am Stat Assoc* 79:871–880. doi:[10.1080/01621459.1984.10477105](https://doi.org/10.1080/01621459.1984.10477105)
- Rousseeuw P, Leroy M (2003) Robust regression and outlier detection. Wiley, New York (ISBN 978-0471488552)
- Salvini D (2008) Konzeption und Entwicklung neuer interaktiver multimedialer Lern- und Arbeitsmethoden für die geodätische Ausgleichsrechnung. PhD thesis, ETH Zürich, Institut für Geodäsie und Photogrammetrie, nr. 17968 (ISBN 978-3-906467-81-8)
- Schlüter W, Behrend D (2007) The international VLBI service for geodesy and astrometry (IVS): current capabilities and future prospects. *J Geod* 81(6–8):379–387. doi:[10.1007/s00190-006-0131-z](https://doi.org/10.1007/s00190-006-0131-z)
- Schubert S, Rood R, Pfaendtner J (1993) An assimilated dataset for Earth science applications. *Bull Am Meteorol Soc* 74(12):2331–2342
- Seitz M, Angermann D, Bloßfeld M, Drewes H, Gerstl M (2012) The 2008 DGF realization of the ITRS: DTRF2008. *J Geod* 86(12):1097–1123. doi:[10.1007/s00190-012-0567-2](https://doi.org/10.1007/s00190-012-0567-2)
- Tesmer V, Steigenberger P, Rothacher M, Böhm J, Meisel B (2009) Annual deformation signals from homogeneously reprocessed VLBI and GPS height time series. *J Geod* 83(10):973–988. doi:[10.1007/s00190-009-0316-3](https://doi.org/10.1007/s00190-009-0316-3)
- Thomas JB (1972) An analysis of long baseline radio interferometry. In: JPL technical report 32-1526, vol VII, pp 37–50
- Thomas JB (1972) An analysis of long baseline radio interferometry, Part II. In: JPL technical report 32-1526, vol VIII, pp 29–38
- Thomas JB (1973) An analysis of long baseline radio interferometry, Part III. In: JPL technical report 32-1526, vol XVI, pp 47–64
- Vennebusch M, Böckmann S, Nothnagel A (2007) The contribution of very long baseline interferometry to ITRF2005. *J Geod* 81(6–8):553–564. doi:[10.1007/s00190-006-0117-x](https://doi.org/10.1007/s00190-006-0117-x)